



UNIVERSITY OF LEEDS

This is a repository copy of *Effects of patient room layout on viral accrument on healthcare professionals' hands*.

White Rose Research Online URL for this paper:  
<https://eprints.whiterose.ac.uk/174610/>

Version: Accepted Version

---

**Article:**

Wilson, AM, King, M [orcid.org/0000-0001-7010-476X](https://orcid.org/0000-0001-7010-476X), López-García, M et al. (4 more authors) (2021) Effects of patient room layout on viral accrument on healthcare professionals' hands. *Indoor Air*. ISSN 0905-6947

<https://doi.org/10.1111/ina.12834>

---

© 2021 John Wiley & Sons A/S. This is the peer reviewed version of the following article: Wilson, A.M., King, M.-F., López-García, M., Clifton, I.J., Proctor, J., Reynolds, K.A. and Noakes, C.J. (2021), Effects of patient room layout on viral accrument on healthcare professionals' hands. *Indoor Air*, which has been published in final form at <https://doi.org/10.1111/ina.12834>. This article may be used for non-commercial purposes in accordance with Wiley Terms and Conditions for Use of Self-Archived Versions. Uploaded in accordance with the publisher's self-archiving policy.

**Reuse**

Items deposited in White Rose Research Online are protected by copyright, with all rights reserved unless indicated otherwise. They may be downloaded and/or printed for private study, or other acts as permitted by national copyright laws. The publisher or other rights holders may allow further reproduction and re-use of the full text version. This is indicated by the licence information on the White Rose Research Online record for the item.

**Takedown**

If you consider content in White Rose Research Online to be in breach of UK law, please notify us by emailing [eprints@whiterose.ac.uk](mailto:eprints@whiterose.ac.uk) including the URL of the record and the reason for the withdrawal request.



[eprints@whiterose.ac.uk](mailto:eprints@whiterose.ac.uk)  
<https://eprints.whiterose.ac.uk/>

1 Effects of patient room layout on viral accrument on healthcare professionals' hands

2 Running title: Effect of patient room layout on viral exposures

3  
4 Amanda M. Wilson<sup>1,2,3\*</sup>, Marco-Felipe King<sup>4</sup>, Martín López-García<sup>5</sup>, Ian J. Clifton<sup>6</sup>,  
5 Jessica Proctor<sup>4</sup>, Kelly A. Reynolds<sup>3</sup>, Catherine J. Noakes<sup>4</sup>

- 6  
7 1. Rocky Mountain Center for Occupational and Environmental Health, University of  
8 Utah, USA  
9 2. Department of Family and Preventive Medicine, School of Medicine, University of  
10 Utah, USA  
11 3. Department of Community, Environment, & Policy, Mel and Enid Zuckerman  
12 College of Public Health, University of Arizona, USA  
13 4. School of Civil Engineering, University of Leeds, UK  
14 5. School of Mathematics, University of Leeds, UK  
15 6. The Leeds Regional Adult Cystic Fibrosis Centre, St. James's University  
16 Hospital, Leeds Teaching Hospital NHS Trust, UK

17  
18 \*Please address correspondence to Amanda M. Wilson, [apfeifer@email.arizona.edu](mailto:apfeifer@email.arizona.edu)

19 Keywords: virus, fomite, exposure, healthcare, human behavior

20  
21 **Funding:** M-F. King and C.J. Noakes were funded by the Engineering and Physical Sciences  
22 Research Council, UK: Healthcare Environment Control, Optimization and Infection Risk  
23 Assessment (<https://HECOIRA.leeds.ac.uk>) (EP/P023312/1). M. López-García was funded by  
24 the Medical Research Council, UK (MR/N014855/1). J. Proctor was funded by EPSRC Centre  
25 for Doctoral Training in Fluid Dynamics at Leeds (EP/L01615X/1).

26  
27 **Code availability:** Under a Creative Commons Zero v1.0 Universal license (CC-BY), code can  
28 be accessed at: [https://github.com/awilson12/room-orientation\\_behavior](https://github.com/awilson12/room-orientation_behavior)

29  
30 **Conflicts of Interest:** None to report.

31  
32 **Ethics Approval:** The study was approved by the NHS Health Research Authority Research  
33 Ethics Committee (London - Queen Square Research Ethics Committee), REF: 19/LO/0301. All  
34 patients and staff involved in this study signed consent forms.

35  
36 **Author contributions:** AM Wilson led the code development, exposure model development,  
37 CFD/human behavior/surface contact model integration, and the manuscript writing. M-F King  
38 co-led CFD/human behavior/surface contact model integration, designed and conducted the  
39 CFD modeling, implementation, and interpretation; led the collection of human behavior data;  
40 contributed to the design of exposure scenarios and model integration methods; and contributed  
41 to manuscript writing. M López-García provided input on modeling methods and interpretation  
42 and contributed to manuscript writing. I Clifton provided medical perspective on interpretation of  
43 results. Jessica Proctor contributed to the collection of human behavior data. Kelly A. Reynolds  
44 provided input on microbial assumptions on the microbial transfer model. Catherine J. Noakes  
45 provided input on the model scenarios and CFD methodology.

46 **Abstract**

47 Healthcare professionals (HCPs) are exposed to highly infectious viruses, such as  
48 norovirus, through multiple exposure routes. Understanding exposure mechanisms will  
49 inform exposure mitigation interventions. The study objective was to evaluate the  
50 influences of hospital patient room layout on differences in HCPs' predicted hand  
51 contamination from deposited norovirus particles. Computational fluid dynamics (CFD)  
52 simulations of a hospital patient room were investigated to find differences in spatial  
53 deposition patterns of bioaerosols for right-facing and left-facing bed layouts. A  
54 microbial transfer model underpinned by observed mock care for three care types  
55 (intravenous therapy (IV) care, observational care, doctors' rounds) was applied to  
56 estimate HCP hand contamination. Viral accrument was contrasted between room  
57 orientation, care type and by assumptions about whether bioaerosol deposition was the  
58 same or variable by room orientation. Differences in sequences of surface contacts  
59 were observed for care type and room orientation. Simulated viral accrument  
60 differences between room types were influenced by mostly by differences in bioaerosol  
61 deposition and by behavior sequences when deposition patterns for the room  
62 orientations were similar. Differences between care types were likely driven by  
63 differences in hand-to-patient contact frequency, with doctors' rounds resulting in the  
64 greatest amount of viral accrument on hands.

65

66 **Practical Implications**

67 Understanding spatial deposition of bioaerosols containing norovirus and the influence  
68 of space on human behavior are crucial to increasing accuracy of predicting exposure

69 on hands and subsequent infection risks from self-inoculation behaviors. As  
70 demonstrated in the simulations in this work, the timing of glove donning/doffing and  
71 hand sanitizer use can have important implications for their ability to protect healthcare  
72 workers, especially considering hand-to-patient contacts. These models can inform  
73 administrative controls, such as training that quantitatively illustrates concepts such as  
74 the importance of proper donning/doffing technique and the 5 moments for hand  
75 hygiene (which include after a patient contact) for lowering occupational microbial  
76 exposures.

## 77 **Introduction**

78 Healthcare professionals (HCPs) face a number of unique occupational hazards  
79 including exposures to infectious agents that may be present in the work environment  
80 due to infected patients, visitors, co-workers or contamination in the environment. In the  
81 U.S., more than 18 million workers are in the healthcare industry, and as this number  
82 continues to increase, HCPs have some of the highest rates of occupationally-related  
83 illness.<sup>1</sup> Worldwide, the prioritization of the health of HCPs has been emphasized due to  
84 increased healthcare demands in response to the COVID-19 pandemic.<sup>2,3</sup> By July 16,  
85 2020, the U.S. Centers for Disease Control and Prevention (CDC) reported HCPs  
86 accounting for approximately 4% (100,570 out of 2.5 million) of U.S. COVID-19 cases.<sup>4</sup>  
87 However, the proportion of cases attributable to HCPs could be higher due to only  
88 having HCP status data for 22% of total reported cases.<sup>4</sup> In a study of 120,075 UK  
89 essential and non-essential workers, HCPs had a 7.43 (95% CI: 5.52, 10.00) times  
90 greater risk of severe COVID-29 relative to non-essential workers.<sup>5</sup> This risk ratio was  
91 greater than that of “social and educational workers” and of “other essential workers”  
92 relative to non-essential workers.<sup>5</sup>

93 Even outside of pandemic conditions, HCPs may be regularly exposed to other  
94 highly infectious agents, such as norovirus, a non-enveloped, single-stranded RNA  
95 enteric virus<sup>6,7</sup> that is generally spread via a fecal-oral pathway and can be transmitted  
96 via person-to-person, fomite, and airborne routes where aerosols are inhaled into the  
97 mouth.<sup>8-10</sup> Healthcare workers have been shown to be at high risk for norovirus  
98 infection during outbreaks in occupational settings.<sup>11</sup> Norovirus infection of HCPs can  
99 lead to not only health risks and loss of time at work but also risks to patients, especially

100 considering the potential for asymptomatic infection and high viral shedding.<sup>11</sup> Analysis  
101 of the burden of norovirus in UK hospitals over a 3 year period suggests an annual  
102 median of 290,000 bed-days were attributable to norovirus, displacing 57,800 other  
103 patients and costing £107.6 million.<sup>12</sup> The same study analyzed reported data on the  
104 impacts on HCPs, estimating that a median of 4,200 members of staff were absent  
105 annual during norovirus outbreaks.

106 While norovirus has been shown to be transmitted via a fomite route, exposure  
107 routes in the environment are often interconnected, where norovirus on fomites may  
108 originate from bioaerosol deposition. Bioaerosols may originate from vomit or fecal  
109 shedding events. In this way, exposures via air, surfaces, and direct person-to-person  
110 contact (such as contacts between HCPs and patients) are a part of a larger system  
111 contributing to exposure.

112 The potential for fomite contamination spread via hand-to-surface contacts,  
113 especially for HCPs, has been a long-recognized mechanism of nosocomial disease  
114 transmission.<sup>13,14</sup> The frequency and sequence of contacts with different surface  
115 types,<sup>15,16</sup> for different care types during simulated vs. actual procedures,<sup>16,17</sup> and the  
116 effect of these differences on microbial exposures have been explored.<sup>18</sup> However, it is  
117 unknown how spatial differences between patient rooms may affect deposition patterns,  
118 hand-to-surface behaviors of healthcare professionals, and subsequent exposures.  
119 Understanding the influence of spatial differences on behavior and contamination  
120 spread via the air-surface interface is important for advancing efforts for developing  
121 environment-specific infection control protocols.

## 122 *Study Objective*

123           The objective of this study was to evaluate the influence of differences in HCP  
124 behavior and differences in airflow and subsequent bioaerosol deposition on surfaces  
125 for two single patient room layouts on norovirus accrument on HCP hands. A  
126 secondary objective was to demonstrate how a calibrated microbial transfer model can  
127 be utilized in exposure modeling. To meet these objectives, an integrated exposure  
128 model composed of a finite volume Navier Stokes computational fluid dynamics (CFD)  
129 model using Lagrangian particle tracking,<sup>19</sup> a human behavior model informed by real-  
130 world data,<sup>17</sup> and a viral transfer model calibrated for representation of transfer of  
131 enteric viruses<sup>20</sup> was developed.

## 132 **Methods**

### 133 *Behavior Observations & Simulation of Behaviors*

134           Hand-to-surface and hand hygiene events (glove donning/doffing and hand  
135 sanitizer use) were recorded for healthcare professionals in single patient rooms  
136 conducting mock IV-care, observational care, or doctors' rounds. A hand-to-surface  
137 contact event was defined as a single hand making physical contact with the object.  
138 Details regarding behavioral observations have been described by King et al.<sup>16</sup> Discrete  
139 Markov chains informed by observed behaviors were used to simulate sequences of  
140 hand-to-surface contacts, glove donning/doffing, or hand hygiene, as has been done in  
141 other healthcare worker behavior modeling.<sup>21</sup>

142           Six transitional probability matrices were created for right- and left-facing rooms  
143 for observational care, IV-drip care, and doctors' rounds using the function  
144 "markovchainFit" from the R statistical software package, *markovchain*. For each

145 probability matrix, behavior states included entrance into patient room, exit from patient  
146 room, use of alcohol gel, hand-to-equipment contact, hand-to-far patient surface  
147 contact, hand-to-near patient surface contact, hand-to-patient contact, doffing of gloves,  
148 donning of gloves, and hand-to-hygiene surface contact. Categories of surfaces  
149 matching these surface type designations for categorizing observed behaviors have  
150 been described previously by King et al. (2020).<sup>17</sup> Transitional probability matrices were  
151 altered so that exit from patient room was an absorbing state and the probability of an  
152 “entrance into patient room” event after the initial entrance was zero.

153         When generating behavior sequences, each sequence began with entrance into  
154 the patient room. New events would be generated until exit from the patient room  
155 occurred. To evaluate the effect of iteration choice on mean accrument on hands over  
156 the number of contacts, mean concentrations on the right hand were compared for  
157 1,000; 5,000; and 10,000 iterations per room type (left- and right-facing) and care type  
158 (IV-care, observational care, doctors’ rounds) combination. There were no notable  
159 differences in mean concentration on the hand over the number of contacts between  
160 results for the 5,000 and 10,000 iteration runs (Supplemental Materials Figures S1-S3).  
161 Therefore, 5,000 iterations were used.

### 162 *Exposure Model Scenarios*

163         In Scenario 1, the same concentrations of norovirus on surfaces were used  
164 regardless of patient bed orientation. Heterogeneity in concentrations between surfaces  
165 was informed by CFD simulations for the right-facing room orientation, and these results  
166 were then used for both the right- and left-facing rooms. Therefore, any differences  
167 between exposures by room orientation or procedure type could then be determined to



168 be behavior driven. In Scenario 2, CFD was used to predict the likely effect of patient  
169 bed orientation and room layout on heterogeneous deposition of bioaerosols on  
170 surfaces of different surface types (near patient vs. far patient surfaces, for example).

### 171 *Changes in Norovirus Concentration on Hands*

172 During the contact,  $k$ , with a surface, a change in norovirus concentration on  
173 either a gloved or ungloved hand was estimated as a function of transfer efficiency ( $\lambda$ , in  
174 hand-to-surface and surface-to-hand directions), fraction of the hand in contact with the  
175 surface ( $S_H$ ), the concentration of norovirus on the surface ( $C_{surface}$ ), and the  
176 concentration of norovirus on the hand before this contact ( $C_{hand,k-1}$ ) (viral  
177 particles/cm<sup>2</sup>) (eq 1), an adapted version of a model by Julian et al. (2009).<sup>22</sup> It was  
178 assumed HCP hands were uncontaminated at the start of care.

179

$$180 \quad C_{hand,k} = C_{hand,k-1} - \lambda S_H (C_{hand,k-1} - C_{surface}) \quad (1)$$

181

182 While asymmetrical transfer efficiencies have been reported for certain  
183 organisms and it has been noted that assuming transfer efficiency is the same in both  
184 directions can result in substantial modeling errors,<sup>23-25</sup> MS2 and PhiX174, enteric  
185 viruses, have been shown to transfer similarly from hand-to-surface and surface-to-  
186 hand.<sup>20,24</sup>

187 Changes in concentration on surfaces were not tracked, as it was assumed that  
188 different portions of the same surface may be contacted and that deposited virus on that  
189 surface was spread homogeneously across the entire surface area. Inactivation of virus  
190 was not incorporated, as non-enveloped viruses can persist in the environment for

191 longer periods relative to the duration of episodes of care. For example, Fedorenko et  
192 al. (2020) demonstrated that MS2 and PhiX174, non-enveloped enteric viruses, in  
193 evaporated saliva microdroplets on a glass surface only reduced by approximately 1  
194  $\log_{10}$  over a 14-hour period for a range of relative humidities.<sup>26</sup> By comparison, observed  
195 mock care episodes used to inform simulated behaviors in this study ranged from 0.6 to  
196 11.7 minutes.<sup>17</sup>

197  
198 *Transfer Efficiency*

199 Values for transfer efficiency ( $\lambda$ ) were informed by a probability distribution  
200 calibrated to the model through previous work relevant for hand-to-surface contacts and  
201 enteric viral exchange between two contaminated surfaces.<sup>20</sup> It is acknowledged that  
202 these transfer efficiencies are not specific to the wide variety of surfaces anticipated in  
203 this exposure scenario. However, to our knowledge, other transfer efficiencies available  
204 in the literature<sup>27,28</sup> are limited in that they do not account for both surfaces being  
205 contaminated. While the first contact in the simulation assumes an uncontaminated  
206 hand contacts a surface, following contacts involve exchange of norovirus between  
207 surfaces and hands. Since this distribution was calibrated for hand-to-surface contacts,  
208 specifically, a different value was used for hand-to-patient contacts.

209 King et al. found that *Escherichia coli* transfer efficiencies for ungloved contacts  
210 (49%, 95% CI = 32-72%) were higher than for gloved contacts (30%, 95% CI=17-  
211 49%).<sup>29</sup> This has been demonstrated for other organisms as well.<sup>23</sup> Transfer efficiency  
212 for a gloved contact was therefore assumed to be 0.61 times smaller than the randomly  
213 sampled transfer efficiency from the posterior distribution of transfer efficiencies from  
214 Wilson et al. (2020).<sup>20</sup>

215 While microbial transfer between hand-to-hand contacts has been demonstrated,  
216 transfer efficiency values were not available for application in the microbial transfer  
217 model. Therefore, we assumed that transfer efficiency between the gloved or ungloved  
218 hand of a healthcare worker and the skin or clothing of a patient could span a wide  
219 range of transfer efficiencies. We assumed a uniform distribution with a minimum of  
220 0.0001 and a maximum of 0.406, as these are minimum and maximum transfer  
221 efficiencies for MS2 reported by Lopez et al. (2013) that capture both nonporous and  
222 porous surfaces under low relative humidity conditions (15-32%).<sup>27</sup>

### 223 *Fraction of Total Hand Surface Area of Contact*

224 Different distributions to describe the fraction of the hand used per hand-to-  
225 surface contact ( $S_H$ ) were used depending upon the contact type. For entrance and exit  
226 from the patient room, it was assumed that an open hand grip would be used.  
227 Therefore, a uniform distribution was randomly sampled with a minimum of 0.10 and a  
228 maximum of 0.21, the minimum and maximum  $S_H$  of left and right hands measured by  
229 AuYeung et al. (2008).<sup>30</sup> For patient contacts, it was assumed that a partial front palm  
230 without fingers up to a full front palm with fingers may be used.<sup>30</sup> Therefore, a uniform  
231 distribution with a minimum of 0.03 and a maximum of 0.25 was randomly sampled,  
232 where these minimum and maximum values were informed by AuYeung et al. (2008).<sup>30</sup>  
233 The fractions of the hand used for partial front palm without finger contact configurations  
234 are similar to those for front partial fingers,<sup>30</sup> so this range includes values that could  
235 represent this configuration as well. For all other contacts it was assumed that various  
236 grip and hand press contact types could be used, aside from hand immersion contacts  
237 described by AuYeung et al. (2008).<sup>30</sup> Therefore, a uniform distribution with a minimum

238 of 0.008 (the minimum of front partial fingers/ 5 fingers to represent a single fingertip  
239 contact) and a maximum of 0.25 (the maximum of full front palm with fingers) were  
240 used.<sup>30</sup>

#### 241 *Glove Donning/Doffing*

242 It was assumed at the start of the simulation that HCPs were not wearing gloves.  
243 If a glove event occurred, this was not donning or doffing specific, but, rather, the  
244 current state was changed from either gloved to ungloved or from ungloved to gloved.  
245 This prevented instances such as a glove donning event following a later glove donning  
246 event without an intermediary doffing event or sequential glove doffing events without  
247 an intermediary donning event. For hand hygiene events, it was ensured that this was  
248 under ungloved conditions. If a hand hygiene event was selected when gloves were on  
249 the hands, a new event was randomly sampled until a non-hand-hygiene event was  
250 selected.

#### 251 *Hand Hygiene Efficacy*

252 When a hand sanitizer event was selected and if gloves were not on, norovirus  
253 concentration on hands was reduced by an efficacy informed by Wilson et al. (2020),  
254 where efficacies with an alcohol-based hand sanitizer were measured with human  
255 norovirus for 30- and 60-second contact times.<sup>31</sup> Due to a low sample size for efficacies  
256 reported by Wilson et al. (2020), a uniform distribution was used with a minimum (0.15  
257  $\log_{10}$ ) and a maximum (2.07  $\log_{10}$ ) informed by minimum and maximum reductions for  
258 the nonresidual alcohol-based hand sanitizer for both 30- and 60-second contact  
259 times.<sup>31</sup> If gloves were on for this hand hygiene moment, a new event was randomly

260 sampled to replace the hand sanitizer event under the assumption that hand sanitizer  
261 would not be applied with gloves on.

### 262 *Infection Risk*

263 Infection risks were estimated to evaluate how differences in viral concentration  
264 on hands would relate to risk differences between care types and room orientations.  
265 Due to lack of sequence data to include hand-to-face contacts within the simulation, a  
266 single hand-to-face contact was assumed at the end of the simulation to estimate an  
267 infection risk based on the concentration on the hands at the end of the episode of care.  
268 Single hand-to-face contacts have been used in other exposure modeling studies to  
269 compare risks between different scenarios.<sup>32</sup> However, it is acknowledged that these  
270 risks do not reflect those of reality, as they do not account for the timing and frequency  
271 of expected hand-to-face contacts and are only using these risks for comparison  
272 purposes.

273 To estimate an infection risk, a viral dose was first estimated by multiplying a  
274 transfer efficiency, hand surface area, and fraction of the total hand surface area to be  
275 used by the concentration on the right or left hand, where either hand had a 50/50  
276 chance of being chosen based on reported lack of differences in contact sequences for  
277 right and left hands in a micro-activity study.<sup>33</sup> If no gloves were on, a transfer efficiency  
278 was randomly sampled from a normal distribution informed by Rusin et al.<sup>28</sup> and left-  
279 and right-truncated at 0 and 1, respectively. If gloves were worn, these transfer  
280 efficiencies were reduced, consistent with how transfer efficiencies for hand-to-fomite  
281 contacts were handled, described above. Total hand surface area for a single hand was  
282 randomly sampled from a uniform distribution (min=445 cm<sup>2</sup>, max=535 cm<sup>2</sup>) informed by

283 Beamer et al. (2015)<sup>34</sup> and the U.S. EPA's Exposure Factors Handbook (2011).<sup>35</sup> It was  
284 assumed a single fingertip or a fraction of the palm would be used for the contact, and  
285 this fraction of total hand surface area that this represents was randomly sampled from  
286 a uniform distribution (min=0.006, max=0.012). The minimum and maximum fractions of  
287 the hand that all fingertips represent reported by AuYeung et al.<sup>30</sup> for adult hands were  
288 divided by 5 to inform the distribution.

289 To relate these doses to infection risk, an approximate beta-Poisson curve was  
290 used, where  $\alpha = 0.104$  and  $\beta = 32.3$  (eq 2)<sup>36</sup>:

$$291 \quad P(\text{infection}) = 1 - \left(1 + \frac{\text{dose}}{\beta}\right)^{-\alpha} \quad (2)$$

292 Although this curve is being used to estimate risks for comparison purposes, it is  
293 acknowledged that multiple dose-response curves for norovirus exist and should be  
294 considered when predicting risks for risk assessments.<sup>36</sup>

### 295 *CFD Methodology*

296 The CFD methodology by King et al. (2013)<sup>19</sup> was closely followed, and CFD  
297 methodology details for this work, specifically, have been explained in other work.<sup>37</sup>  
298 Briefly, a steady state simulation assuming isothermal conditions and natural ventilation  
299 from three windows open 10 cm with an air exchange rate of 6 was modeled using  
300 Fluent v.19.4 (ANSYS, Canonsburg, PA, USA). The door (pressure outlet) had a  
301 surface area of 1.9 m<sup>2</sup> while the large window (velocity inlet) had a surface area of 0.18  
302 m<sup>2</sup> and the small windows (velocity inlets) each had a surface area of 0.08 m<sup>2</sup>. A  
303 velocity mesh sensitivity analysis was conducted with three sequentially size-halved cell  
304 sizes. A hex-dominant mesh with 4 cm element size and 2 cm cells was used for the  
305 bulk volume and close to surfaces, respectively. We used a k-omega transition shear

306 stress transport turbulence model with standard omega wall function formulation. A  
307 point near the patient mouth was set as the inert water particle injection site, where  
308 particles were injected at a velocity of 1.9 m/s, in part informed by Tang et al. (2013).<sup>38</sup>  
309 This is based on breathing due to a lack of data on velocity and aerosols associated  
310 with vomiting events, but is considered as representative of a small aerosol source from  
311 a person. We assume that large droplets and splashes would be cleaned immediately  
312 post event, so are concerned about the surface contamination that may occur sometime  
313 later following the event. Addressing aerosol emissions due to breathing also increases  
314 the generalizability of this work, providing insights into how emissions of respiratory  
315 viruses via breathing may deposit on surfaces and contribute to fomite-mediated  
316 exposure routes as well. However, experimental data used to calibrate the microbial  
317 transfer model used in this integrated model more appropriately represent enteric  
318 viruses, such as norovirus. The particle size range (0.14 to 8.13  $\mu\text{m}$ ) was informed by  
319 Alsved et al. (2020).<sup>39</sup> This range reflects a range of aerosols in which Alsved et al.  
320 (2020) detected norovirus.<sup>39</sup> The particle diameter remained constant throughout the  
321 simulation, assuming that all particles were their fully evaporated size. Deposition of  
322 particles on surfaces were then tracked using a Lagrangian particle methodology with  
323 discrete random walk and trap boundary condition on surfaces, including the walls.

324 The fraction of injected particles that landed on specific surface types were  
325 related to expected viral concentrations on surfaces by estimating a number of viral  
326 particles to be released by a patient, informed by Alsved et al. (2020) and the U.S.  
327 Environmental Protection Agency's Exposure Factors Handbook (2011).<sup>35,39</sup> The  
328 fraction of virus expected to land on each respective surface was then calculated,

329 divided by the total surface area to obtain viral particles/cm<sup>2</sup>. Surface areas of surfaces  
330 are listed in Table S1. Sizes of particles were not tracked upon deposition, meaning that  
331 the fraction of deposited particles does not account for differences in particle size or  
332 virus concentrations across ranges of particle sizes. However, the distribution of particle  
333 sizes in this study was low, with most of the distribution of sizes being below 5 µm,  
334 meaning we would not expect as much error due to assuming homogeneous deposition  
335 of particle sizes across surfaces as if we considered a range of larger aerosol sizes in  
336 which larger aerosols may settle considerably faster than fine aerosols <5 µm.

337 For the right-facing room orientation, estimated particle deposition on the desk  
338 was used to inform the concentration anticipated on far patient and hygiene area  
339 surfaces. For the left-facing room orientation, surface concentrations on far patient and  
340 hygiene area surfaces were informed by the concentration on the wall. For the right-  
341 facing room orientation, near patient and equipment surface concentrations were  
342 informed by estimated particles deposited on the side table, bed, and chair, while for  
343 left-facing rooms, near patient and equipment surface concentrations were also  
344 informed by deposition on the desk in addition to these other surfaces.

345 For both room orientations, particles deposited on the patient were used to  
346 inform concentrations on the patient. The “in” and “out” event, entrance and exit from  
347 the patient room, respectively, involved contact with the door handle. In this case, it was  
348 assumed that concentrations on the door handle were zero since the focus of this study  
349 was on fomite-mediated exposures as a result of particle deposition alone.



350 *Exposure Model Sensitivity Analysis*

351 Spearman correlation coefficients were calculated to quantify monotonic  
352 relationships between model inputs and the mean and maximum concentrations on  
353 hands. Since some parameters, such as transfer efficiency, surface concentration, and  
354 the fraction of the hand used for a contact, varied by contact, the mean value of these  
355 parameters per iteration was used. Spearman correlation coefficients were also  
356 calculated to investigate relationships between input parameters, since some inputs  
357 were related, where a greater amount of patient contacts could relate to a greater mean  
358 transfer efficiency since larger transfer efficiencies were used for hand-to-patient  
359 contacts than for hand-to-surface contacts, for example. Since some relationships  
360 between model inputs and mean or maximum viral concentration on hands may not be  
361 monotonic, scatter plots were also visually inspected.

362 *Particle Deposition Sensitivity Analysis*

363 In addition to the baseline model involving 6 ACH and the windows acting a  
364 velocity inlet and the door acting as a pressure outlet, particle deposition patterns for  
365 other scenarios were explored: the door acting as a velocity inlet and windows acting as  
366 a pressure outlet, the small windows acting as velocity inlets and the large window  
367 acting as a pressure outlet, and exploring 2.5 ACH and 10 ACH in addition to 6 ACH.  
368 Mean viral concentrations on hands for left- and right-facing rooms were then compared  
369 for these 9 scenarios (3 ACHs x 3 velocity inlet, pressure outlet scenarios).

370 **Results**

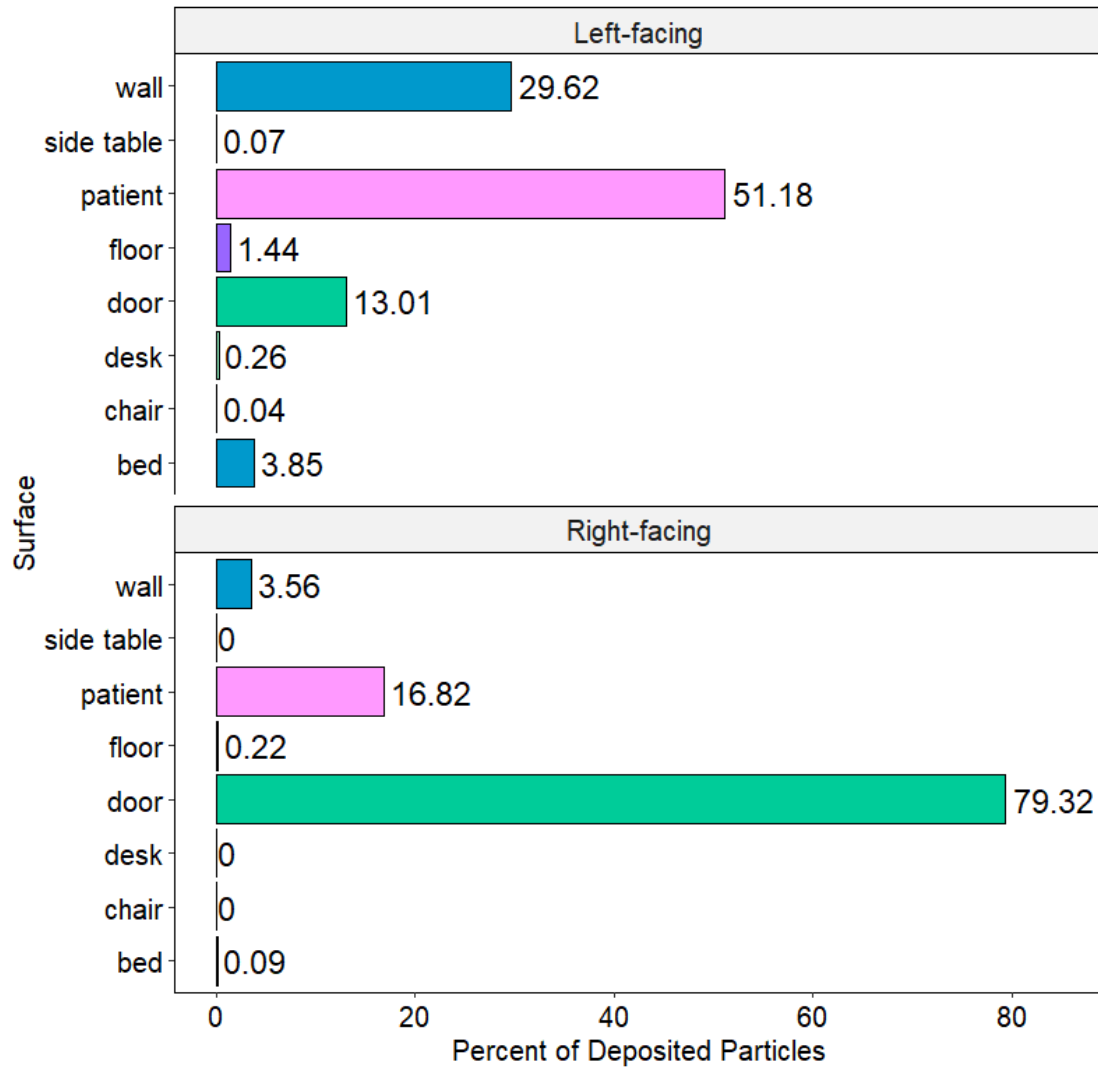
371 *Deposition*

372

373                   The predicted deposition of particles on surfaces between the left- and  
374 right-facing rooms in the primary model (6 ACH, windows as velocity inlets, door as  
375 pressure outlet) were notably different (Figure 1). The left-facing room resulted in  
376 51.18% of emitted particles depositing on the patient, while the right-facing room only  
377 resulted in 16.82% (Figure 1). High passage of particles through the door surfaces was  
378 expected, such as for the right-facing room (79.32% of particles passing through the  
379 door) as this was the airflow outlet and windows were velocity inlets. While not within  
380 the scope of this exposure assessment, this would suggest would be those that would  
381 be extracted by ventilation in the corridor or potentially to another patients room.  
382 Viewing the particle tracks, it can be seen that in the right-facing room, the incoming air  
383 from the open windows may be directing air from the injection point near the patient  
384 mouth out the door, whereas in the left-facing room, particles appear to remain in the  
385 room longer, leaving more opportunities for deposition on the patient, floor and  
386 surrounding surfaces (Figures 1 and 2).

387                   Slightly more deposition occurred on the floor for the left-facing room (1.44%)  
388 than for the right-facing room (0.22%). While no interactions with the floor were modeled  
389 in this study, this may have infection control implications beyond the focus of this work,  
390 as pathogens have been detected on floors,<sup>40</sup> and floors make contact with some  
391 fomites and can participate in wider facility contamination via shoe movement and  
392 portable equipment.<sup>41</sup>

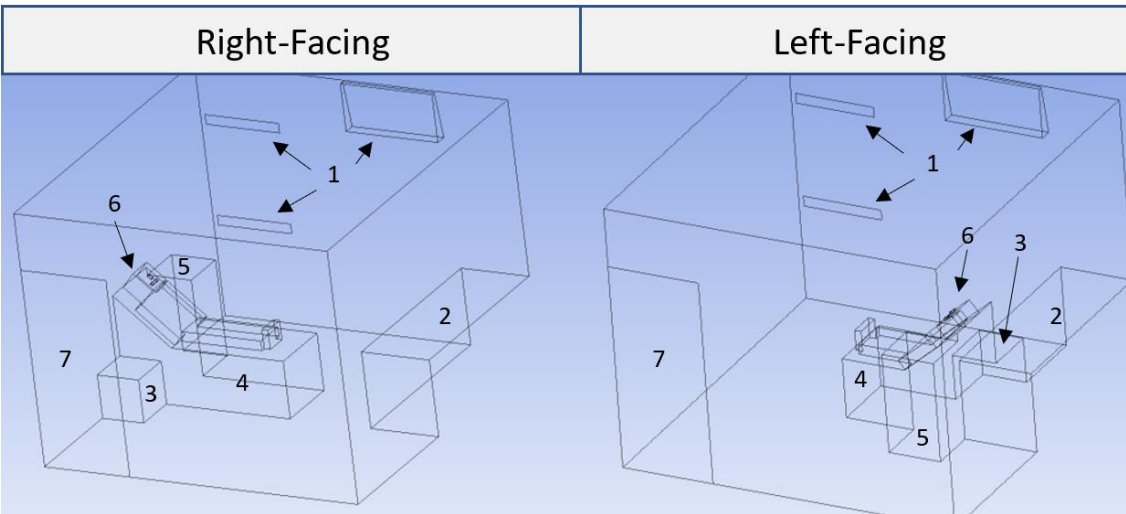
393



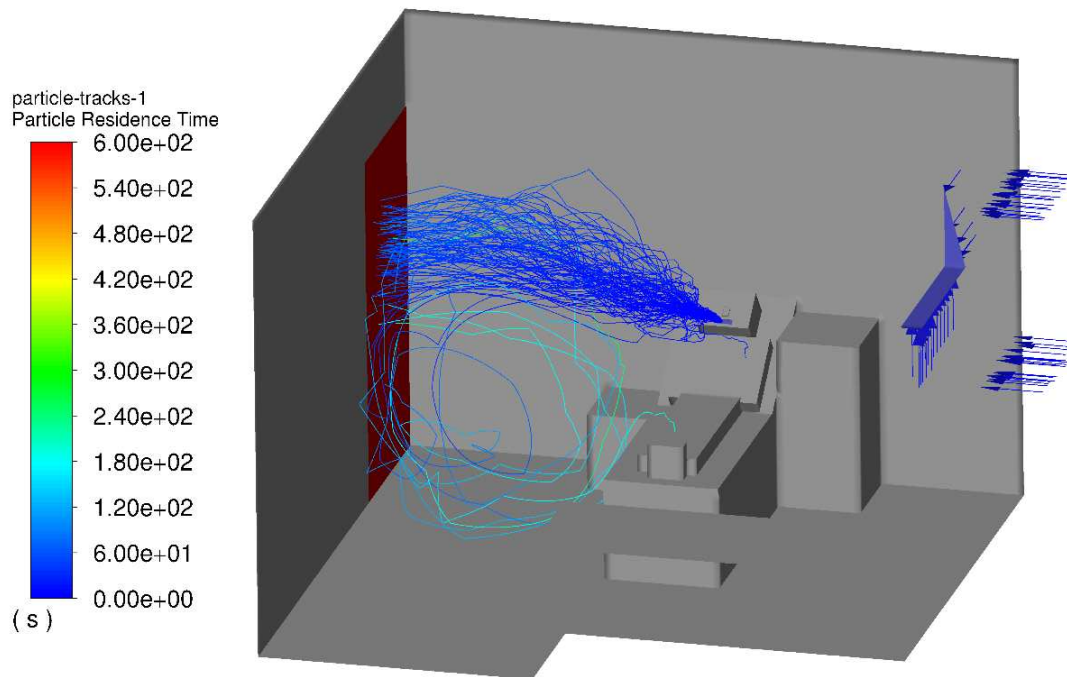
394  
 395  
 396  
 397  
 398

**Figure 1.** Deposition and surface areas of surfaces in the CFD modeling for left- and right-facing rooms

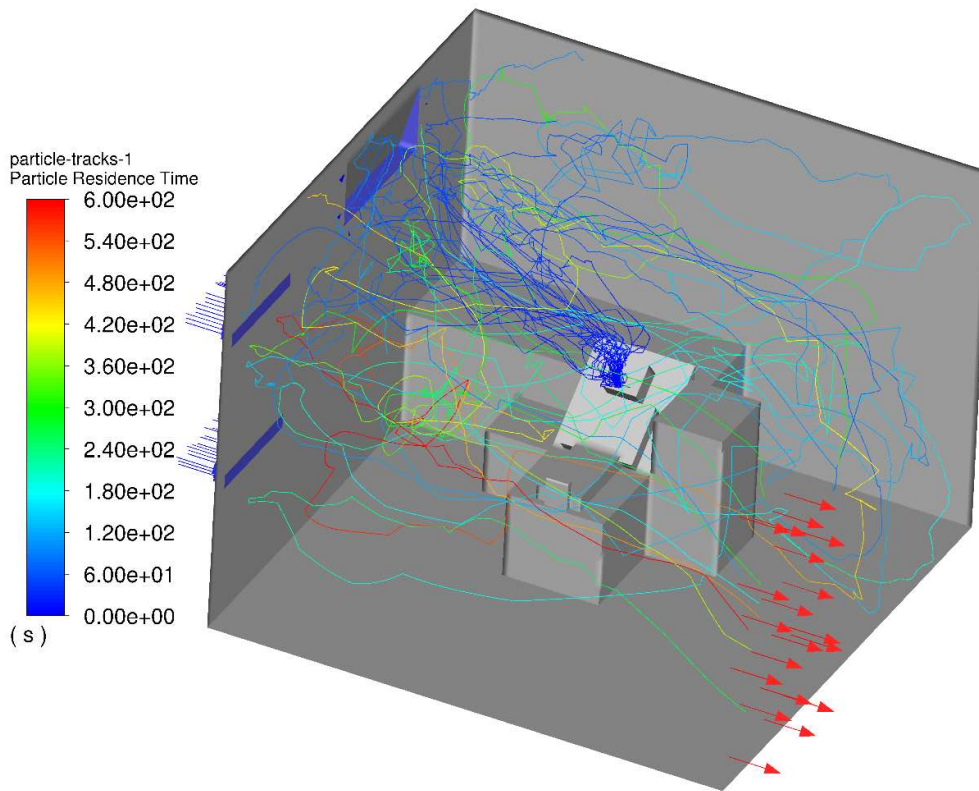
**A**



**B**



C



399 **Figure 2.** Right- and left-facing room A) Geometry (1=windows, 2=desk, 3=chair,  
400 4=bed, 5=side table, 6=patient, 7=door) and particle tracking illustrations colored by  
401 residence time for the B) right-facing room and C) left-facing room  
402

403

404

### *Simulated Behaviors*

405

406

407

408

409

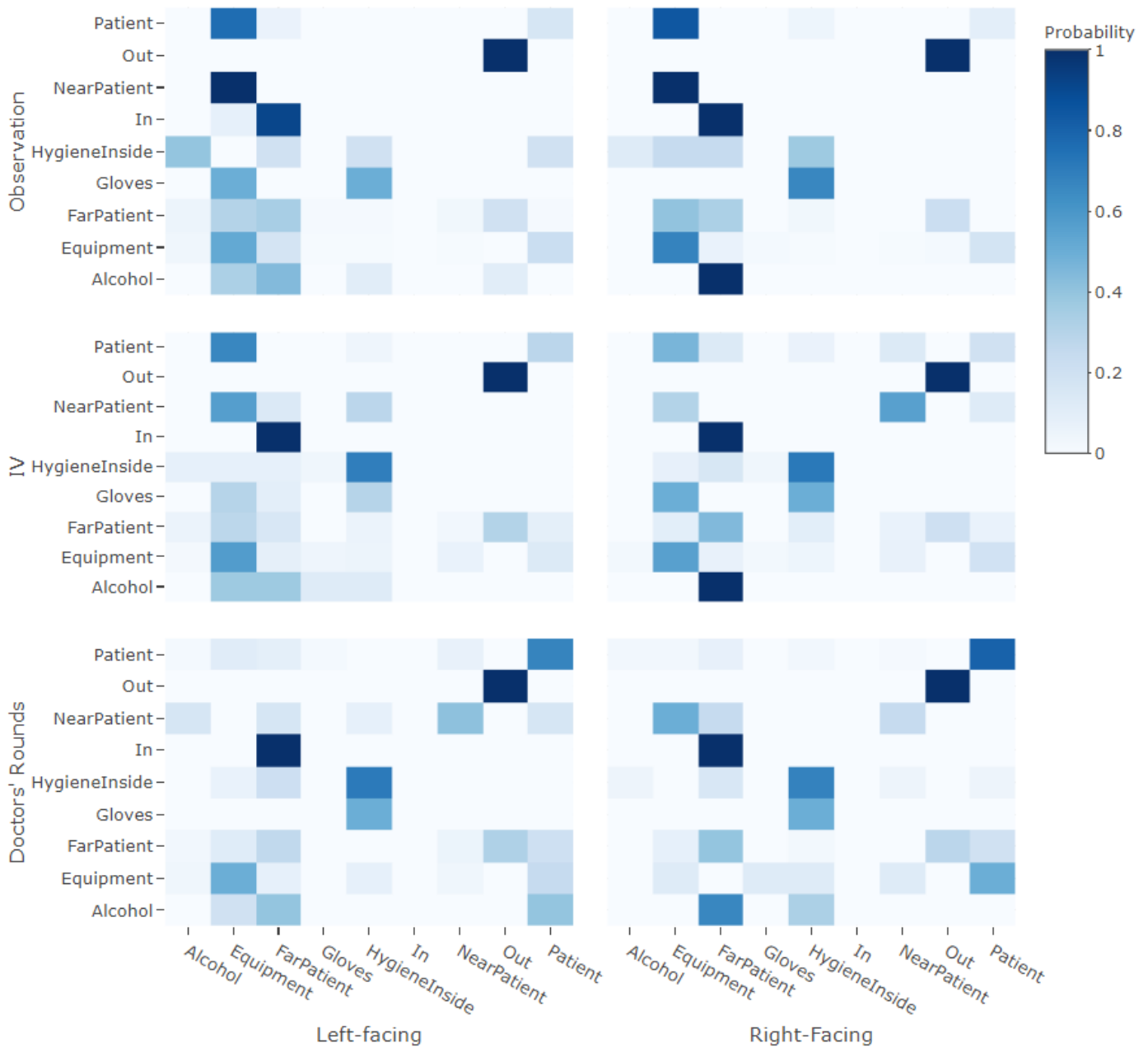
410

The transitional probability matrices for doctors' rounds, regardless of room orientation, demonstrated a high probability of repetitive contacts with the patient (Figure 3), where the left- and right-facing orientation probabilities of the next event being a hand-to-patient contact given a current hand-to-patient contact were 0.68 and 0.81, respectively. This is also reflected in the proportions of events that make up all

411 events in simulations for each room orientation and care type, where patient contacts  
412 made up 32% and 42% for contacts in doctors' rounds in left- and right-facing rooms,  
413 respectively (Figure 4).

414 When investigating how often glove donning or doffing events were resampled,  
415 which occurred if glove donning occurred when gloves were already donned or of glove  
416 doffing events occurred when gloves were not already donned, the frequency of these  
417 occurrences depended upon care type and room orientation. For left-facing rooms, this  
418 happened in 15.7% of IV care, 2.8% of doctors' rounds, and 5.1% of observational care  
419 episodes that were simulated. For right-facing rooms, this happened in 3.6% of IV care,  
420 3.1% of doctors' rounds, and 8.1% of observational care episodes that were simulated.

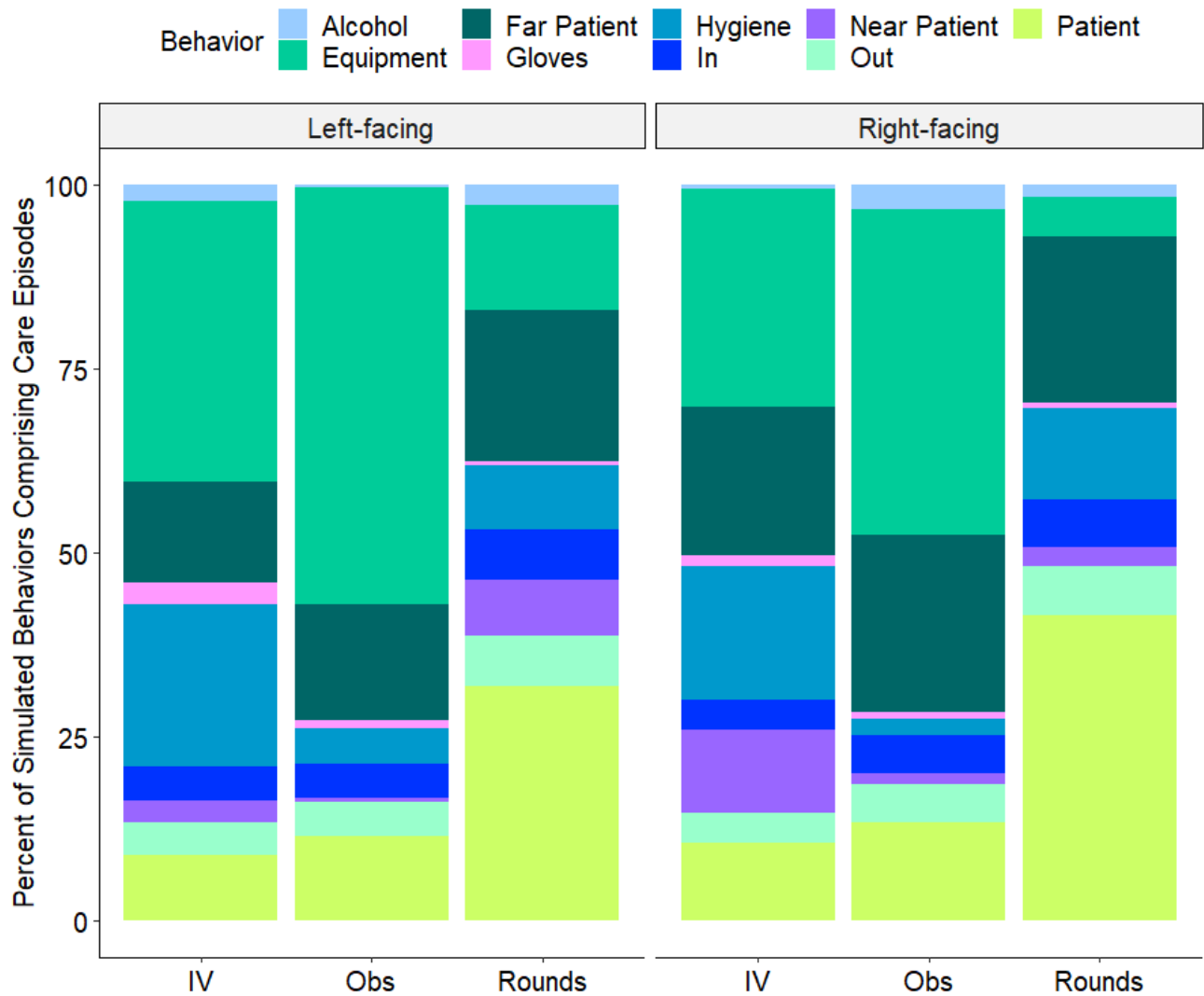
421 All transitional probabilities involved relatively high probabilities of a transition  
422 from entrance into the patient room to contact with a far-patient surface (Figure 3),  
423 ranging from 0.92 to 1, and this contact type accounted for similar proportions of total  
424 events among all care type and room orientation combinations (Figure 4). Contact with  
425 the door was considered a far patient contact in informing transitional probability  
426 matrices, so this may explain the high probability of a far patient contact following  
427 entrance into the room. Contacts with equipment comprised a large proportion of events  
428 for left- and right-facing observational care, where this contact type accounted for 57%  
429 and 44% of events in left- and right-facing rooms, respectively (Figure 4). This is  
430 consistent with many high probability transitions from a given surface or event to a  
431 hand-to-equipment contact for observational care, especially for left-facing rooms  
432 (Figure 3).



433  
 434  
 435  
 436  
 437  
 438  
 439  
 440

**Figure 3.** Heatmap of transitional probability matrices for two room orientations (left- and right-facing) and three care types (IV-care, observational care, and doctors' rounds)\*

\*These matrices represent transition from row-to-column, where probabilities in rows add up to 1.



442 **Figure 4.** Proportion of simulated behaviors comprising each contact event type per  
 443 care type (IV-care, observational care, and doctors' rounds) and room orientation (left-  
 444 and right-facing)  
 445

446  
 447  
 448 *Viral Accrue ment*

449  
 450 When differences in viral deposition on surfaces and differences in behaviors due  
 451 to room orientation were accounted for, notable differences in viral accrue ment on  
 452 hands between the two room orientations were seen for doctors' rounds and less so for  
 453 IV-care and observational care (Figure 5). For doctors' rounds, left-facing rooms



454 resulted in more viral accrument on hands overall than right-facing rooms, where  
455 accrument for IV-care and observational care were more similar for the right-facing  
456 than for left-facing room (Figure 5).

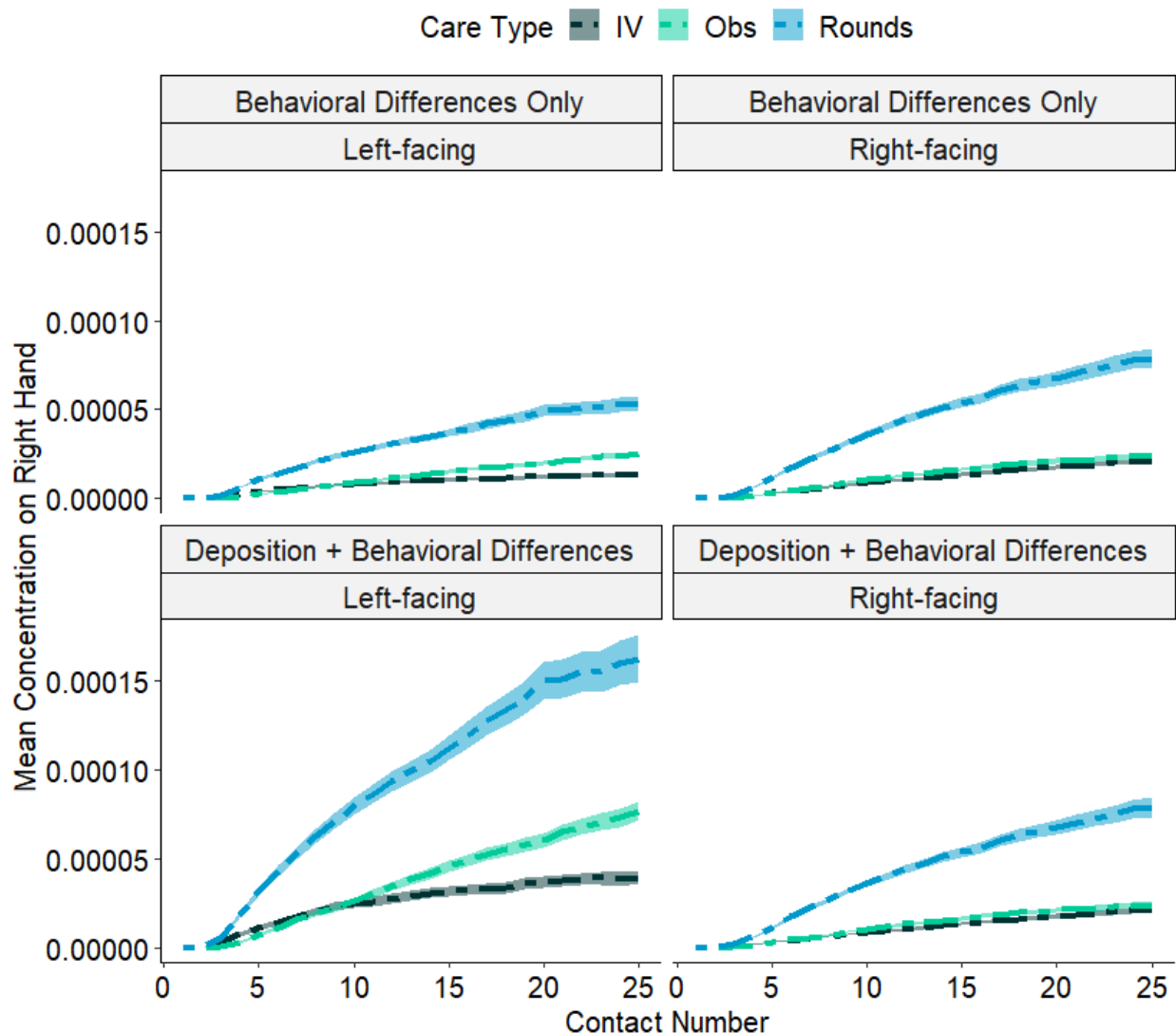
457 For left-facing rooms, these differences translated to doctors' rounds resulting in  
458 240% and 43% greater mean infection risks relative to IV-care and observational care,  
459 respectively. Mean infection risks for the three care types were  $3.0 \times 10^{-7}$  (doctors'  
460 rounds),  $8.8 \times 10^{-8}$  (IV-care), and  $2.1 \times 10^{-7}$  (observational care). For right-facing rooms,  
461 these differences translated to 122% and 186% greater mean infection risks for doctors'  
462 rounds relative to IV-care and observational care, respectively. Mean infection risks for  
463 the three care types were  $1.4 \times 10^{-7}$  (doctors' rounds),  $6.3 \times 10^{-8}$  (IV-care), and  $4.9 \times 10^{-8}$   
464 (observational care).

465 When comparing infection risks between room orientations, mean infection risk  
466 for doctors' rounds in left-facing rooms was 114% greater relative to right-facing rooms.  
467 IV-care in left-facing rooms resulted in a mean infection risk that was 40% greater  
468 relative to right-facing rooms. For observational care, left-facing rooms resulted in a  
469 mean infection risk that was 329% greater relative to right-facing rooms.

470 It should be noted that these are infection risks for only one hand-to-face contact  
471 directly after an episode of care. In some simulated cases, a hand-to-face contact was  
472 made with a freshly donned glove, resulting in a zero dose. More data are needed to  
473 accurately capture infection risks due to self-inoculation behaviors and the effects of  
474 personal protective equipment (PPE) on these behaviors.

475 When deposition differences were removed so that only behavioral differences  
476 between room orientations were accounted for, differences in accrument on hands

477 between left- and right-facing room layouts were diminished but with slightly more  
478 accrument on the hands for the right-facing orientation than for the left-facing  
479 orientation (Figure 5). In both right- and left-facing rooms regardless of deposition  
480 differences, the least amount of viral accrument occurred for IV care episodes, while  
481 doctors' rounds resulted in the most accrument (Figure 5). This is consistent with  
482 doctors' rounds resulting in the greatest mean infection risks, described above. In  
483 addition to increased risks for HCPs, greater viral accrument on hands could lead to  
484 higher risks to patients as well, as doctors' rounds have larger proportions of patient  
485 contacts compared to other care types (Figure 4). The number of iterations used to  
486 inform the mean concentration on hands per contact number can be seen in Figure S4.  
487



488  
 489  
 490  
 491  
 492  
 493  
 494  
 495  
 496  
 497  
 498  
 499  
 500  
 501  
 502

**Figure 5.** Comparison of accretion on hands over the number of contacts\*

\*Mean  $\pm$  SD of virus concentration (viral particles/cm<sup>2</sup>) on a single hand, compared by care type (IV-care, observational care, doctors' rounds), room orientation (left-facing, right-facing) and assumptions regarding differences in viral concentrations on surfaces and behaviors based on room orientation. Deposition + Behavioral plots demonstrate the effects of differences in surface concentrations influenced by deposition differences between the left- and right-facing rooms along with differences in transitional probability matrices for simulating sequences of behaviors for the two room orientations. "Behavioral differences only" plots demonstrate the effects of deposition patterns for the right-facing room used for both right- and left-facing rooms so that differences in accretion are only representative of differences in transitional probability matrices for the care types by room orientation. Concentrations here represent average concentrations estimated to be on hands at any given simulated moment, explaining

503 why some concentrations (viral particles/cm<sup>2</sup>) multiplied by the cm<sup>2</sup> of a hand would be  
504 less than 1, indicating a less than 100% chance of a viral particle being present on the  
505 hand.

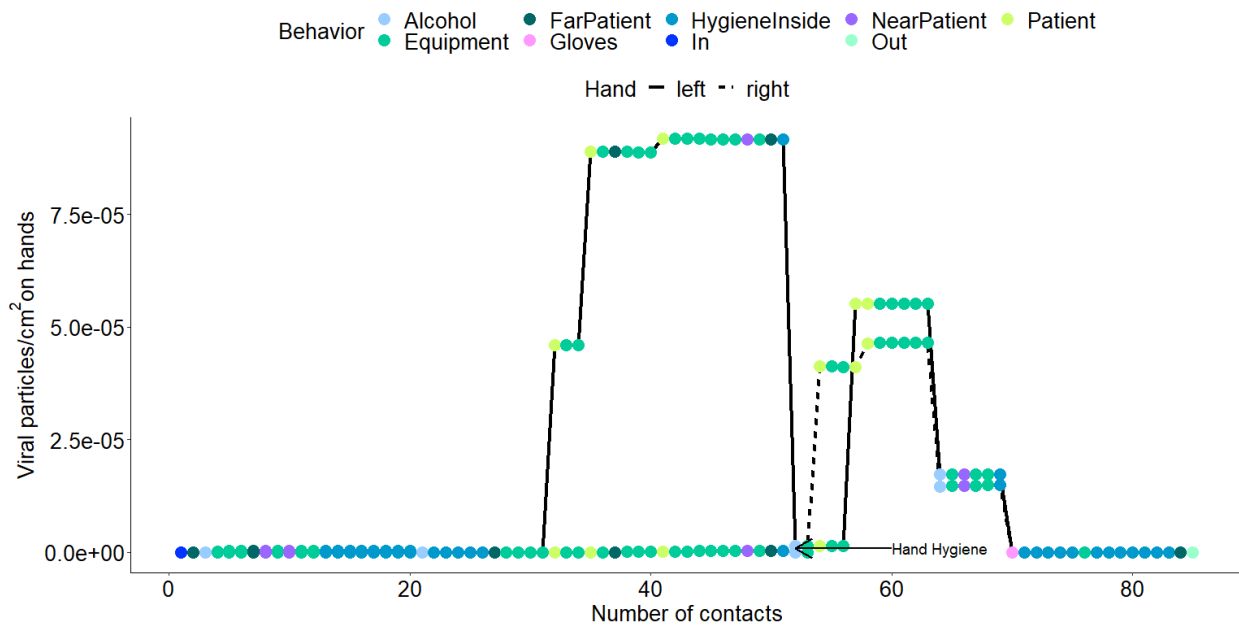
506  
507

### 508 *Viral Loss from Hands*

509

510 Because the microbial transfer model in this study assumes transfer of virus in  
511 both directions, loss of virus from the hands occurs depending upon a concentration  
512 gradient between the hand (gloved or ungloved) and the surface in contact (eq 1). Use  
513 of hand sanitizer is one mechanism by which accruement on hands can be lost (Figure  
514 6). This is especially advantageous following contacts that resulted in fast viral  
515 accruement, such as contacts with a patient, demonstrated in a plot of viral accruement  
516 for one model iteration in Figure 6.

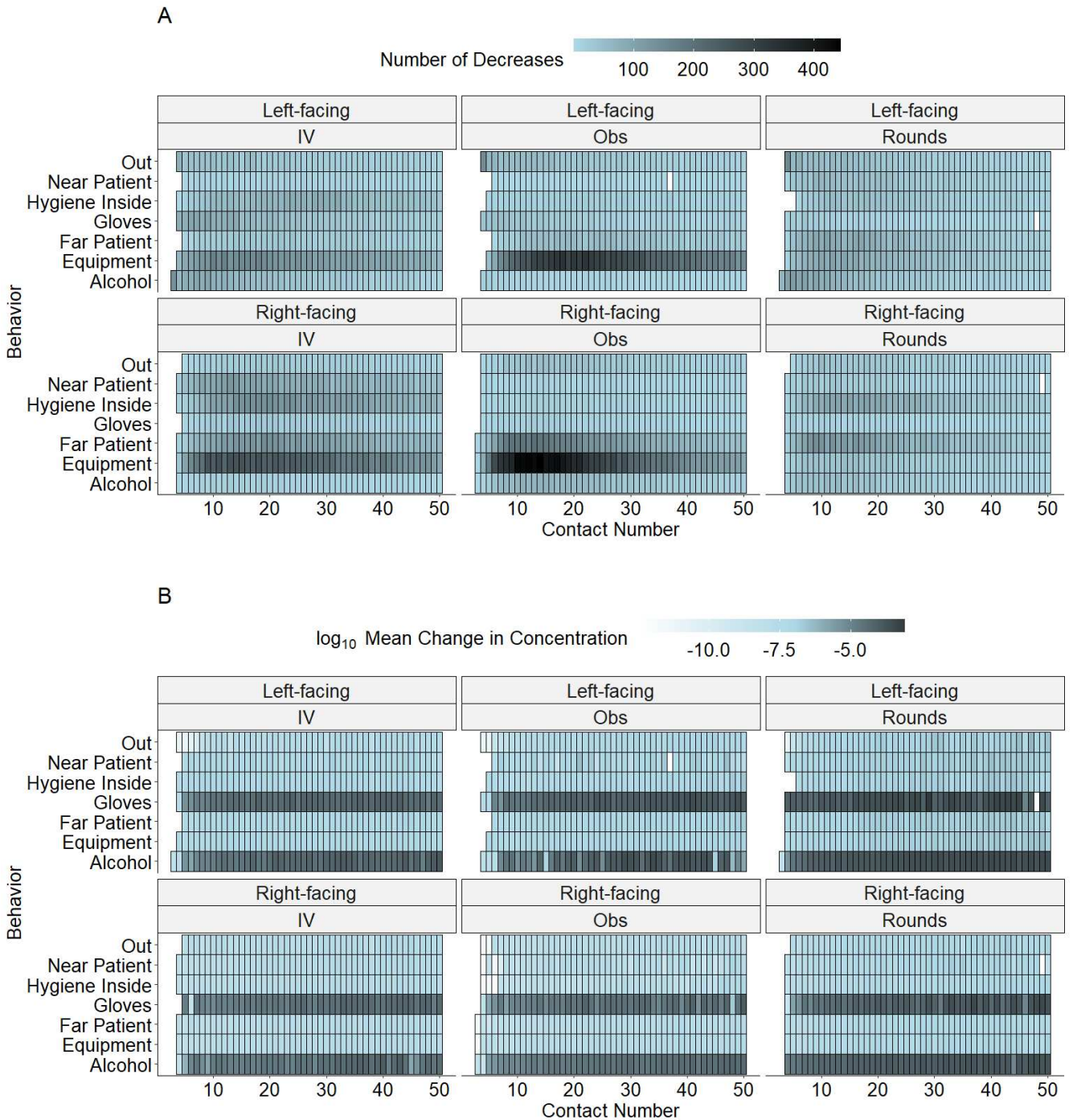
517



518  
519  
520  
521

**Figure 6.** Example of large increases in accruement due to hand-to-patient contacts and decreases due to use of alcohol-based hand sanitizer

522 While the use of gloves can be an effective means for lowering potential  
523 exposures, glove events did not account for most of the losses from hands that  
524 occurred over the contacts (Figure 7A), in part potentially due to the low frequency of  
525 glove events (Figure 4). More frequent events, such as contacts with equipment  
526 surfaces, especially during observational care, contributed to more instances of viral  
527 loss from the hands than most of the glove or even alcohol hand sanitizer events  
528 (Figure 7A). However, this is related to the number of iterations in which events at  
529 specific moments in the behavior sequence resulted in loss. It does not account for the  
530 magnitude of loss. When observing the  $\log_{10}$  of the mean change in concentrations  
531 during these moments of loss, alcohol hand sanitizer and glove events result in larger  
532 magnitudes of loss than hand-to-surface events (Figure 7B), even if they contribute to  
533 loss of viral accrument less frequently (Figure 7A). The magnitude of viral loss  
534 attributable to the alcohol hand sanitizer and glove donning/doffing events is consistent  
535 regardless of room orientation or care type, emphasizing their importance and  
536 relevance as infection control strategies.



537 **Figure 7.** Evaluation of moments of viral loss through **A.)** Number of simulations in  
 538 which an event resulted in a loss of concentration on hands and **B.)** Log<sub>10</sub> mean change  
 539 in concentration for moments of loss associated with these events\*

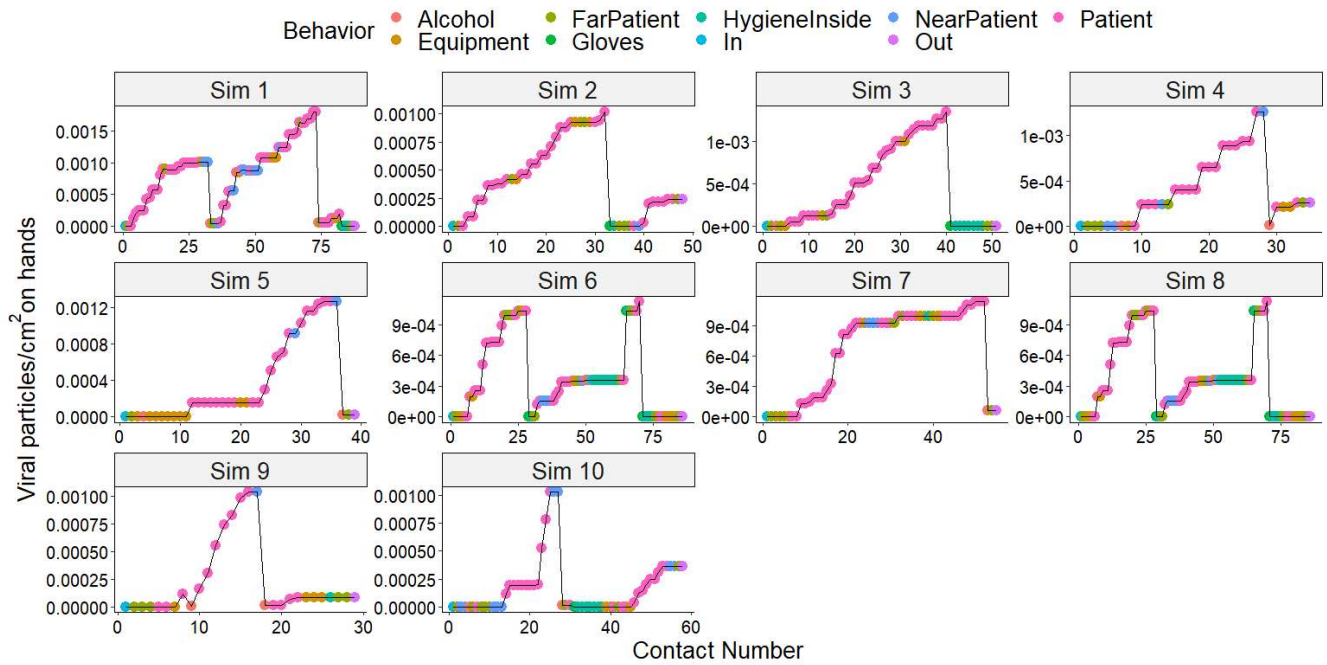
540

541 \*These results reflect simulations in which both bioaerosol deposition and human  
 542 behaviors differences for the two room orientations (left- and right-facing)

543

544  
545  
546  
547  
548  
549

The ten greatest viral losses occurred during doctors' rounds simulations. The behavior sequences for these simulations were characterized by viral accrument over multiple hand-to-patient contacts followed by alcohol hand sanitizer use or a change in glove status (donning or doffing) (Figure 8).



550

551 **Figure 8.** Simulations with the greatest instances of viral loss\*

552 \*Viral particles/cm<sup>2</sup> on hands shows the combined concentrations on the right and left  
553 hands over the number of contacts in the simulation. These results reflect simulations in  
554 which both bioaerosol deposition and human behavior differences for the two room  
555 orientations (left- and right-facing)

556

557 A greater number of hand sanitizer events per total number of events in a care

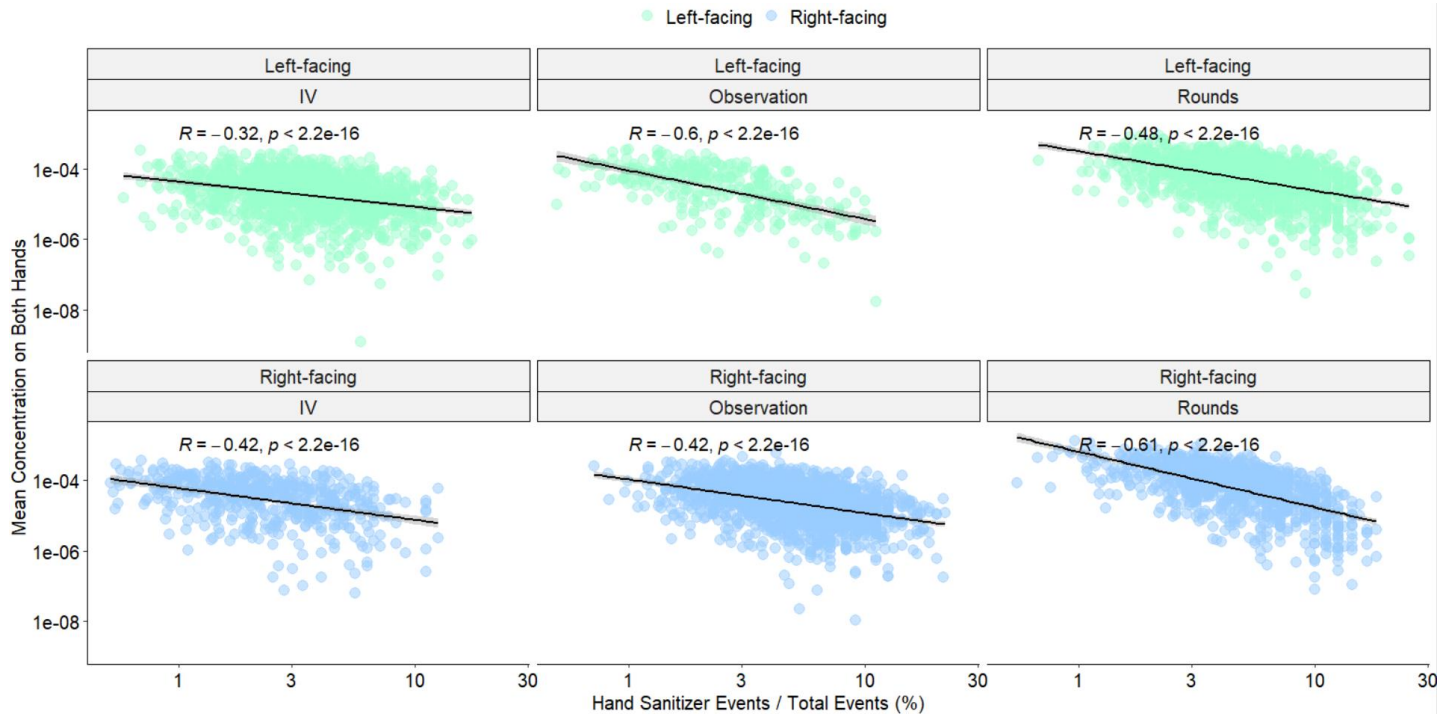
558 episode was associated with smaller mean concentrations on the hands, where the

559 log<sub>10</sub> concentration had a negative linear relationship with log<sub>10</sub> percent of events

560 represented by hand sanitizer events (Figure 9). This negative relationship was

561 consistent across room orientations and care types (Figure 9).

562 While a greater number of hand sanitizer events per total events was associated  
 563 with decreases in mean concentration on hands, the effect of the number of hand  
 564 sanitizer events alone was less clear due to instances in which there was a high number  
 565 of hand sanitizer events for a care episode longer than other episodes with more  
 566 opportunities for viral accrument on hands. Similarly, some care episodes contained  
 567 no hand hygiene moments but were composed of only 3 contact events, resulting in  
 568 smaller mean concentrations on the hands relative to simulations in which there were  
 569 more hand sanitizer events but also more surface contact events. This emphasizes the  
 570 importance of considering hand hygiene in the form of hygiene consistency over the  
 571 duration of an entire care episode as opposed to evaluating hand hygiene merely based  
 572 on frequency.



573  
 574 **Figure 9.** Mean concentration on both hands (viral particles/cm<sup>2</sup>) vs. the percent of total  
 575 events that are hand sanitizer events for scenarios\*  
 576



577 \*Spearman correlation coefficients and p values calculated for simulations in which at  
578 least 1 hand hygiene event and at least 1 hand-to-patient contact occurred are reported  
579 per care type and room orientation combination. Concentrations here represent average  
580 concentrations estimated to be on hands at any given simulated moment, explaining  
581 why some concentrations (viral particles/cm<sup>2</sup>) multiplied by the cm<sup>2</sup> of a hand would be  
582 less than 1, indicating a less than 100% chance of a viral particle being present on the  
583 hand.

584  
585

#### 586 *Exposure Model Sensitivity Analysis*

587 Mean and maximum concentrations on hands had strong relationships with  
588 transfer efficiency, with Spearman correlation coefficients ranging from 0.77-0.82,  
589 depending up on the care type and room orientation (Figures S5-S10). While transfer  
590 efficiency is traditionally not an influential parameter in similar models, it had a strong  
591 relationship with patient contacts ( $\rho=0.84$  for IV-care in left-facing rooms, for example,  
592 Figure S5) due to assumed greater transfer efficiencies with patient skin as opposed to  
593 with surfaces. For all room orientations and care types with the primary CFD model, the  
594 number of patient contacts had the second strongest relationship with mean and  
595 maximum concentrations on hands, with surface concentrations being the strongest  
596 (Figures S5-S10). When observing distributions of log<sub>10</sub> mean concentrations on hands,  
597 notable differences in magnitude and shape of distributions can be seen for simulations  
598 in which at least 1 patient contact was made versus none (Figure S11). Scatter plots  
599 can be seen in supplementary materials, Figures S12-S22.

#### 600 *Particle Deposition Sensitivity Analysis*

601 Notable differences were seen in particle deposition patterns (Figures S23-S25)  
602 and subsequent accrument on hands between left- and right-facing rooms between the  
603 ACH and the inlet/outlet scenarios (Figures S26-S28). Regardless of ACH, the left-

604 facing orientation resulted in more particle deposition on the patient than for the right-  
605 facing orientation when the windows were the velocity inlets and the door was a  
606 pressure outlet and when the windows were velocity inlets and pressure outlets (Figures  
607 S23-S25). However, when the windows were the pressure outlets and the door was a  
608 velocity inlet, the fractions of particles deposited on the patient were more similar for  
609 left- and right-facing rooms (Figures S23-25). When deposition on the patient was more  
610 similar, such as for 6 ACH and the window as the pressure outlet and door as the  
611 pressure inlet (Figure S26C), greater viral accrument was observed for doctors' rounds  
612 for the right-facing rooms as opposed to left-facing. This was also observed when the  
613 effect of differences in bioaerosol deposition were removed, such as in the primary  
614 model (6 ACH, door as pressure outlet, windows as velocity inlets), where doctors'  
615 rounds for the right-facing room resulted in slightly more viral accrument than for the  
616 left-facing rooms when the same bioaerosol deposition pattern was used (Figure 5).

617 In some cases, the ACH did appear to affect which room orientation resulted in  
618 greater viral accrument on hands for doctors' rounds for the same inlet and outlet  
619 conditions. For example, assuming 2.5 or 6 ACH and the windows acting as pressure  
620 outlets and velocity inlets resulted in greater viral accrument on hands for left-facing  
621 rooms (Figures S26B and S28B) while for 10 ACH the viral accrument was slightly  
622 larger for right-facing rooms (Figure S27B). Despite differences between left- and right-  
623 facing orientations and effects of ACH, doctors' rounds remained the care type that  
624 resulted in the greatest viral accrument regardless of ACH or inlet/outlet conditions.  
625 The effect of having the mouth as another inlet in addition to having an injection point  
626 near the patient mouth was also explored for one of the ventilation scenarios, and it did

627 impact the fraction of particles exiting the door and depositing on the wall but did not  
628 greatly influence the fraction of deposition on the patient surface (data not shown).  
629 Since the fraction of deposition on patients appears to be driving differences in between  
630 room orientations, it is anticipated that treating the mouth as an additional inlet would  
631 not have greatly influenced the results. However, variability in emission characteristics  
632 should be further explored in future work.

633

## 634 **Discussion**

### 635 *Key Findings and Generalizability*

636 This study illustrates that the location of the patient and furniture, alone, could  
637 have effects on both the patterns of bioaerosol deposition on surfaces and also on  
638 healthcare workers' micro-activity (second-by-second) behaviors, where room ACH and  
639 flow direction can affect the magnitudes of difference in exposures between room  
640 layouts. Aside from differences in bioaerosol deposition, human behavioral differences  
641 between room layouts were also observed, possibly influenced by training. For  
642 example, in UK hospitals, doctors are trained to approach the patient from the right. In  
643 the right-facing room orientation, getting to the right side of the patient may take more  
644 maneuvering around furniture than in a left-facing room orientation (Figure 2). Greater  
645 travel time to the patient may result in more opportunities for hand-to-surface or hand-  
646 to-patient contacts. The deposition pattern will be determined by the particular  
647 ventilation flow in a room, and the results in this study are specific to the room scenarios  
648 modelled. However it serves to illustrate that a simple change in the location of  
649 furnishing can change the likely pattern of deposition when the ventilation conditions are

650 kept the same, with implications for pathogen accrument on hands (Figures S23-S28).  
651 Further exploration of other ventilation conditions, room orientations, and behaviors for  
652 other care types can further elucidate the influence of room orientations on exposures  
653 and subsequent risks.

654 Behavioral differences and some differences in bioaerosol deposition between  
655 room orientations were seen (Figures 1, 3 and 4), and there were differences in mean  
656 infection risks due to single hand-to-face contacts at the end of care episodes. Infection  
657 risk estimates should be further explored with scenario-specific hand-to-face contact  
658 frequencies as opposed to assuming a single hand-to-face contact. Additionally, the use  
659 of both hands for a hand-to-fomite contact as opposed to use of a single hand and use  
660 of the right vs. the left hand was not explored. It is possible that use of the right vs. the  
661 left hand or the use of both hands vs. a single hand could be procedure-specific. Further  
662 development of this work will involve more granularity regarding hand dominance and  
663 both vs. single hand touches in addition to using observations containing self-  
664 inoculation moments during or after care episodes to estimate infection risks.

665 A notable difference in behaviors between care types was contacts with patients,  
666 where doctors' rounds involved more patient contacts, regardless of room orientation  
667 (Figure 4). Differences in the number of particles deposited on patients appeared to  
668 drive differences in viral accrument on hands for left- and right-facing room orientations  
669 (Figures 5, S23-S28). Because contacts with the patient were frequent and the patient  
670 generally had greater fractions of bioaerosol deposition than other surface types, patient  
671 contacts likely drove differences in viral accrument between care types over the course  
672 of multiple contacts, where greater viral accrument was seen for doctors' rounds

673 (Figure 5). This rationale is also supported by a strong monotonic relationship between  
674 number of patient contacts and mean viral concentration on hands ( $\rho = 0.88$  for doctors'  
675 rounds in left-facing rooms, Figure S9).

676 These hand-to-patient contacts were not only frequent (Figure 4) but also  
677 repetitive for doctors' rounds (Figure 2). This is an important distinction, because  
678 repetitive contacts created opportunities for fast viral accrument relative to hand-to-  
679 patient contacts spread out over the course of an episode of care. This phenomenon  
680 can be seen in simulations in which greatest viral losses due to alcohol hand sanitizer  
681 use or glove donning/doffing occurred (Figures 7B and Figure 8), despite the fact that  
682 other events, such as contacts with equipment, more frequently contributed to viral  
683 losses from hands (Figure 7A).

684 Overall, an increased rate of hand sanitizer events was related to a decrease in  
685 mean viral concentrations on hands for all care types and room orientations (Figure 9).  
686 However, there were instances where hand sanitizer was applied after contacts with  
687 surfaces that did not result in large viral accrument, where the sanitizer did less to  
688 lower exposure. This can be seen in Figure 6 where an early alcohol hand sanitizer  
689 behavior occurred before several hand-to-patient contacts that resulted in large  
690 increases in viral concentration on hands, later decreased by another hand sanitizer  
691 event (Figure 6). The timing of glove doffing is also important, where, when gloves are  
692 worn, viral accrument via repetitive hand-to-patient contacts can be removed when  
693 gloves are doffed, therefore lowering opportunities for large doses via self-inoculation.  
694 However, after a glove doffing event, if more hand-to-patient contacts are made,  
695 potential risks of self-inoculation are increased. It is possible a healthcare worker may

696 more readily make a hand-to-face contact based on a perception of lower contamination  
697 on hands and lower risk. The effects of personal protective equipment (PPE) use and  
698 sequences of high-risk contacts on self-inoculation frequency should be further  
699 explored.

#### 700 *Limitations*

701 While the CFD model in this work was not experimentally validated, natural  
702 ventilation models are notoriously difficult to validate, and previous versions of single  
703 patient hospital room CFD models that informed this model have been validated.<sup>19</sup> The  
704 model presented in the paper is designed to show how simple changes to a room can  
705 influence the likely deposition pattern and hence the subsequent infection risk, rather  
706 than to accurately model a particular room. Deposition differences between the two  
707 room orientations are not representative of true differences under a variety of air flow or  
708 weather conditions and are constrained to assumptions used in the CFD modeling such  
709 as wind direction and velocity. Additionally, thermal effects were not included and  
710 resuspension was not addressed due to uncertainty regarding anticipated amounts of  
711 resuspension during hand-to-surface contacts, the force variability of contacts, and lack  
712 of information regarding walking patterns in the room that could contribute to  
713 resuspension of particles deposited on the floor. Changes in natural ventilation  
714 velocities and influence of thermal effects should also be explored to investigate how  
715 these parameters affect differences in exposures or infection risks between room  
716 orientations.

717 Despite these limitations, the approach we utilized accomplished the objective of  
718 exploring how differences in deposition patterns influenced by room layout may affect

719 healthcare workers' exposures to pathogens following bioaerosol deposition on surfaces  
720 and are therefore non-trivial. Open room doors throughout the day are a frequent  
721 feature of UK hospitals during summer months due to overheating,<sup>42</sup> suggesting that the  
722 scenarios using the door as a velocity inlet or pressure outlet are more applicable under  
723 warm conditions. Future work could involve exploring more real-world scenarios and  
724 chamber studies to measure particle deposition patterns and further evaluate the  
725 contribution of deposition differences to exposure and infection risk differences with the  
726 end goal of informing patient room design and furniture placement.

727         In these simulations, it was assumed that deposition of bioaerosols across an  
728 individual surface was homogeneous. Concentration changes on surfaces were  
729 therefore not tracked, as any fraction of the surface could be touched during a contact  
730 and the same area of the surface may not be touched. This is untrue for the door  
731 handle, but this surface was assumed to have a viral concentration of zero, as the focus  
732 of this exposure modeling study was fomite-mediated exposures as a result of  
733 bioaerosol deposition alone. It is likely that deposition is heterogeneous both between  
734 objects and on each individual object. Further granularity of deposition on high touch  
735 areas of surfaces vs. low touch areas will improve accuracy of exposure models and  
736 provide insights into areas to focus surface cleaning and disinfection. It should be noted  
737 that incorporating this level of detail in exposure models would arguably only be useful if  
738 this same level of detail were available in human behavior data, including which parts of  
739 objects are more commonly touched than others. This approach would also offer  
740 opportunities to incorporate grip-specific hand configurations to more accurately capture  
741 the surface area of the hand that was used.<sup>30</sup>

742           Additionally, transfer efficiencies used here originated from a fingertip-to-surface  
743 contact scenario.<sup>20</sup> While the fingertip or “fingerpad” is often used in transfer efficiency  
744 studies,<sup>24,27,43</sup> transfer efficiency variability by area of the hand used would provide more  
745 contact-specific data to further inform the integration of microbial transfer and human  
746 behavior models. In chemical transfer efficiency contexts, hand presses and fingertip  
747 presses have been used.<sup>44,45</sup> Characterizing what part of the hand is used for self-  
748 inoculation moments would also be important, as loading on the palm but hand-to-face  
749 contact with the fingertip may not result in exposure. Assuming viral loading on the  
750 hands is homogeneous across the hands may over- or under-estimate doses and  
751 subsequent infection risks.

## 752 *Conclusions*

753           This study demonstrates with exposure modeling that doctors’ rounds may pose  
754 greater exposure and infection risks to healthcare workers than IV-care and  
755 observational care, due to faster viral accrument on hands due to a greater frequency  
756 of hand-to-patient contacts. Differences between room orientations in fomite-mediated  
757 exposures via deposited bioaerosols may be a function of changes in human behavior  
758 (different sequences of hand-to-surface contacts) and differences in bioaerosol  
759 deposition. This indicates that bioaerosols and ventilation design could have  
760 implications for not only inhalation exposures but also fomite-mediated exposures,  
761 especially considering the effects of room layout on room- and care type-specific hand-  
762 to-surface contact behaviors. Further expansion of integrated exposure models  
763 incorporating behaviors related to dose, such as self-inoculation, will allow for risk-  
764 informed engineering controls and room design to limit the frequency of hand-to-surface



765 contacts with surfaces experiencing greater bioaerosol deposition. This work also allows  
766 for evaluation of other interventions lower in the hierarchy of controls, including use of  
767 PPE and hand sanitizer. As demonstrated in the simulations in this work, the timing of  
768 glove donning/doffing and hand sanitizer use can have important implications for their  
769 ability to protect healthcare workers, especially considering hand-to-patient contacts.  
770 These models can inform administrative controls, such as training that quantitatively  
771 illustrates concepts such as the importance of proper donning/doffing technique and the  
772 5 moments for hand hygiene (which include after a patient contact)<sup>39</sup> for lowering  
773 occupational microbial exposures.

774

775

776 **References**

777

- 778 1. The National Institute for Occupational Safety and Health (NIOSH). Healthcare Workers.  
779 <https://www.cdc.gov/niosh/topics/healthcare/default.html>. Published 2017. Accessed  
780 September 28, 2020.
- 781 2. Chirico F, Nucera G, Magnavita N. COVID-19: Protecting Healthcare Workers is a  
782 priority. *Infect Control Hosp Epidemiol*. 2020. doi:10.1017/ice.2020.148
- 783 3. Bellizzi S, Fiamma M, Arru L, Farina G, Manca A. COVID-19: The daunting experience of  
784 healthcare workers in Sardinia , Italy. *Infect Control Hosp Epidemiol*. 2020:1-2.  
785 doi:10.1017/ice.2020.149
- 786 4. Hughes MM, Groenewold MR, Lessem SE, et al. Update: Characteristics of Health Care  
787 Personnel with COVID-19 — United States, February 12–July 16, 2020. *Morb Mortal*  
788 *Wkly Rep*. 2020;69(1364-1368). doi:http://dx.doi.org/10.15585/mmwr.mm6938a3external  
789 icon
- 790 5. Mutambudzi M, Niedwiedz C, Macdonald EB, et al. Occupation and risk of severe  
791 COVID-19: prospective cohort study of 120 075 UK Biobank participants. *Occup Environ*  
792 *Med*. 2020:1-8. doi:10.1136/oemed-2020-106731
- 793 6. Centers for Disease Control and Prevention. Norovirus. 2020.  
794 <https://www.cdc.gov/norovirus/lab/virus-classification.html>. Accessed September 28,  
795 2020.
- 796 7. Robilotti E, Deresinski S, Pinsky BA. Norovirus. *Clin Microbiol Rev*. 2015;28(1):134-164.  
797 doi:10.1128/CMR.00075-14
- 798 8. Lopman B. *Global Burden of Norovirus and Prospects for Vaccine Development.*; 2015.  
799 <https://www.cdc.gov/norovirus/downloads/global-burden-report.pdf>.
- 800 9. Xiao S, Tang JW, Li Y. Airborne or fomite transmission for norovirus? A case study  
801 revisited. *Int J Environ Res Public Health*. 2017;14(12). doi:10.3390/ijerph14121571
- 802 10. Kirby AE, Streby A, Moe CL. Vomiting as a symptom and transmission risk in norovirus  
803 illness: Evidence from human challenge studies. *PLoS One*. 2016;11(4):e0143759.  
804 doi:10.5061/dryad.sk800
- 805 11. Sabrià A, Pintó RM, Bosch A, et al. Norovirus shedding among food and healthcare  
806 workers exposed to the virus in outbreak settings. *J Clin Virol*. 2016;82:119-125.  
807 doi:10.1016/j.jcv.2016.07.012
- 808 12. Sandmann FG, Shallcross L, Adams N, et al. Estimating the Hospital Burden of  
809 Norovirus-Associated Gastroenteritis in England and Its Opportunity Costs for  
810 Nonadmitted Patients. *Clin Infect Dis*. 2018;67:693-700. doi:10.1093/cid/ciy167
- 811 13. Kampf G, Löffler H, Gastmeier P. Hand hygiene for the prevention of nosocomial  
812 infections. *Dtsch Arztebl*. 2009;106(40):649-655. doi:10.3238/arztebl.2009.0649
- 813 14. Pittet D. Hand hygiene: From research to action. *J Infect Prev*. 2017;18(3):100-102.  
814 doi:10.1177/1757177417705191
- 815 15. Smith SJ, Young V, Robertson C, Dancer SJ. Where do hands go? An audit of sequential  
816 hand-touch events on a hospital ward. *J Hosp Infect*. 2012;80(3):206-211.  
817 doi:10.1016/j.jhin.2011.12.007
- 818 16. King MF, Noakes CJ, Sleigh PA, Bale S, Waters L. Relationship between healthcare  
819 worker surface contacts, care type and hand hygiene: an observational study in a single-  
820 bed hospital ward. *J Hosp Infect*. 2016;94(1):48-51. doi:10.1016/j.jhin.2016.05.003
- 821 17. King M-F, Wilson AM, Lopez-Garcia M, et al. Why is mock care not a good proxy for  
822 predicting hand contamination during patient care? *J Hosp Infect*. 2021;109:44-51.
- 823 18. King M-F, Wilson AM, Weir MH, et al. Modelling the risk of SARS-CoV-2 infection through  
824 PPE doffing in a hospital environment. *medRxiv*. 2020.  
825 doi:10.1101/2020.09.20.20197368

- 826 19. King M, Noakes CJ, Sleigh PA. Bioaerosol deposition in single and two-bed hospital  
827 rooms: A numerical and experimental study. *Build Environ.* 2013;59:436-447.  
828 doi:10.1016/j.buildenv.2012.09.011
- 829 20. Wilson AM, King M-F, López-García M, et al. Evaluating a transfer gradient assumption in  
830 a fomite-mediated microbial transmission model using an experimental and Bayesian  
831 approach. *J R Soc Interface.* 2020;17(167):20200121. doi:10.1098/rsif.2020.0121
- 832 21. King MF, Noakes CJ, Sleigh PA. Modeling environmental contamination in hospital  
833 single- and four-bed rooms. *Indoor Air.* 2015;25(6):694-707. doi:10.1111/ina.12186
- 834 22. Julian TR, Canales RA, Leckie JO, Boehm AB. A model of exposure to rotavirus from  
835 nondietary ingestion iterated by simulated intermittent contacts. *Risk Anal.*  
836 2009;29(5):617-632.
- 837 23. Greene C, Vadlamudi G, Eisenberg M, Foxman B, Koopman J, Xi C. Fomite-fingerpad  
838 transfer efficiency (pick-up and deposit) of *Acinetobacter baumannii* - With and without a  
839 latex glove. *Am J Infect Control.* 2015;43(9):928-934. doi:10.1016/j.ajic.2015.05.008
- 840 24. Julian TR, Leckie JO, Boehm AB. Virus transfer between fingerpads and fomites. *J Appl*  
841 *Microbiol.* 2010;109(6):1868-1874. doi:10.1111/j.1365-2672.2010.04814.x
- 842 25. Greene C, Ceron NH, Eisenberg MC, et al. Asymmetric transfer efficiencies between  
843 fomites and fingers: Impact on model parameterization. *Am J Infect Control.*  
844 2018;46(6):620-626. doi:10.1016/j.ajic.2017.12.002
- 845 26. Fedorenko A, Grinberg M, Orevi T, Kashtan N. Virus survival in evaporated saliva  
846 microdroplets deposited on inanimate surfaces. *bioRxiv.* 2020.  
847 doi:10.1101/2020.06.15.152983
- 848 27. Lopez GU, Gerba CP, Tamimi AH, Kitajima M, Maxwell SL, Rose JB. Transfer efficiency  
849 of bacteria and viruses from porous and nonporous fomites to fingers under different  
850 relative humidity. *Appl Environ Microbiol.* 2013;79(18):5728-5734.  
851 doi:10.1128/AEM.01030-13
- 852 28. Rusin P, Maxwell S, Gerba C. Comparative surface-to-hand and fingertip-to-mouth  
853 transfer efficiency of gram-positive bacteria, gram-negative bacteria, and phage. *J Appl*  
854 *Microbiol.* 2002;93(4):585-592.
- 855 29. Hefzy EM, Wegdan AA, Abdel Wahed WY. Hospital outpatient clinics as a potential  
856 hazard for healthcare associated infections. *J Infect Public Health.* 2016;9(1):88-97.  
857 doi:10.1016/j.jiph.2015.06.015
- 858 30. AuYeung W, Canales RA, Leckie JO. The fraction of total hand surface area involved in  
859 young children's outdoor hand-to-object contacts. *Environ Res.* 2008;108(3):294-299.  
860 doi:10.1016/j.envres.2008.07.010
- 861 31. Wilson AM, Reynolds KA, Jaykus LA, Escudero-Abarca B, Gerba CP. Comparison of  
862 estimated norovirus infection risk reductions for a single fomite contact scenario with  
863 residual and nonresidual hand sanitizers. *Am J Infect Control.* 2019;48(5):538-544.  
864 doi:10.1016/j.ajic.2019.09.010
- 865 32. Ryan MO, Haas CN, Gurian PL, Gerba CP, Panzl BM, Rose JB. Application of  
866 quantitative microbial risk assessment for selection of microbial reduction targets for hard  
867 surface disinfectants. *Am J Infect Control.* 2014;42(11):1165-1172.  
868 doi:10.1016/j.ajic.2014.07.024
- 869 33. Beamer PI, Luik CE, Canales RA, Leckie JO. Quantified outdoor micro-activity data for  
870 children aged 7 – 12-years old. *J Expo Sci Environ Epidemiol.* 2012;22(1):82-92.  
871 doi:10.1038/jes.2011.34
- 872 34. Beamer PI, Plotkin KR, Gerba CP, Sifuentes LY, Koenig DW, Reynolds KA. Modeling of  
873 human viruses on hands and risk of infection in an office workplace using micro-activity  
874 data. *J Occup Environ Hyg.* 2015;12(4):266-275. doi:10.1080/15459624.2014.974808
- 875 35. U.S. Environmental Protection Agency. *Exposure Factors Handbook 2011 Edition*  
876 *(EPA/600/R-09/052F)*. Washington, DC; 2011.

877 <https://cfpub.epa.gov/ncea/risk/recordisplay.cfm?deid=236252>.

878 36. Van Abel N, Schoen ME, Kissel JC, Meschke JS. Comparison of Risk Predicted by  
879 Multiple Norovirus Dose–Response Models and Implications for Quantitative Microbial  
880 Risk Assessment. *Risk Anal.* 2016;37(2):245-264. doi:10.1111/risa.12616

881 37. Wilson AM, King M-F, Lopez-Garcia M, et al. Integrating CFD and exposure modeling for  
882 estimating viral exposures at the air-surface interface. *AIAA Aviat Forum Expo.*  
883 2020:Under review.

884 38. Tang JW, Nicolle AD, Klettner CA, et al. Airflow dynamics of human jets: Sneezing and  
885 breathing - potential sources of infectious aerosols. *PLoS One.* 2013;8(4):e59970.  
886 doi:10.1371/journal.pone.0059970

887 39. Alsveld M, Fraenkel C-J, Bohgard M, et al. Sources of Airborne Norovirus in Hospital  
888 Outbreaks. *Clin Infect Dis.* 2019:1-6. doi:10.1093/cid/ciz584

889 40. Rashid T, Vonville H, Hasan I. Mechanisms for floor surfaces or environmental ground  
890 contamination to cause human infection: a systematic review. *Epidemiol Infect.*  
891 2017;145(2):347-357. doi:10.1017/S0950268816002193

892 41. Deshpande A, Cadnum JL, Fertelli D, et al. Are hospital floors an underappreciated  
893 reservoir for transmission of health care-associated pathogens? *Am J Infect Control.*  
894 2017;45(3):336-338.

895 42. Gough H, Faulknall-mills S, King M, Luo Z. Assessment of Overheating Risk in  
896 Gynaecology Scanning Rooms during Near-Heatwave Conditions: A Case Study of the  
897 Royal Berkshire Hospital in the UK. *Int J Environ Res Public Health.* 2019;16(8):3347.  
898 doi:10.3390/ijerph16183347

899 43. King MM-F, López-García M, Atedoghu KP, et al. Bacterial transfer to fingertips during  
900 sequential surface contacts with and without gloves. *Indoor Air.* April 2020.  
901 doi:10.1111/ina.12682

902 44. Sahmel J, Hsu EI, Avens HJ, Beckett EM, Devlin KD. Estimation of hand-to-mouth  
903 transfer efficiency of lead. *Ann Work Expo Heal.* 2015;59(2):210-220.

904 45. Hubal EAC, Suggs JC, Nishioka G, Ivancic WA. Characterizing residue transfer  
905 efficiencies using a fluorescent imaging technique. *J Expo Anal Environ Epidemiol.*  
906 2005;15(3):261-270. doi:10.1038/sj.jea.7500400

907

908

909

910

911  
912  
913  
914  
915  
916  
917  
918  
919  
920  
921  
922  
923  
924  
925  
926  
927  
928  
929  
930  
931  
932

Supplemental Materials for:

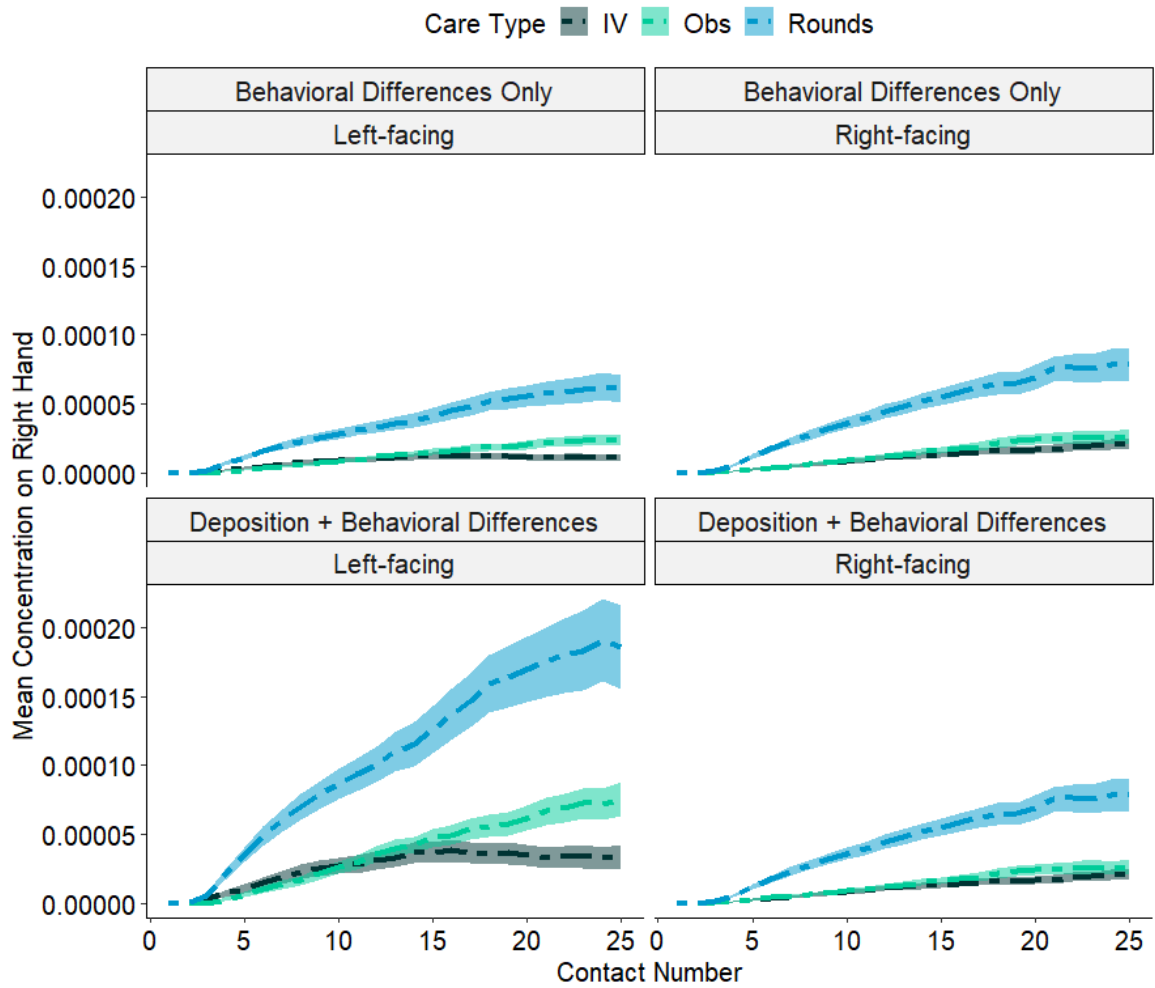
Effects of patient room layout on viral accrument on healthcare professionals' hands

Amanda M. Wilson<sup>1,2\*</sup>, Marco-Felipe King<sup>3</sup>, Martín López-García<sup>4</sup>, Ian Clifton<sup>5</sup>, Jessica Proctor<sup>3</sup>, Kelly A. Reynolds<sup>2</sup>, Catherine J. Noakes<sup>3</sup>

1. Rocky Mountain Center for Occupational and Environmental Health, University of Utah, USA
2. Department of Community, Environment, & Policy, Mel and Enid Zuckerman College of Public Health, University of Arizona, USA
3. School of Civil Engineering, University of Leeds, UK
4. School of Mathematics, University of Leeds, UK
5. The Leeds Regional Adult Cystic Fibrosis Centre, St. James's University Hospital, Leeds Teaching Hospital NHS Trust, UK

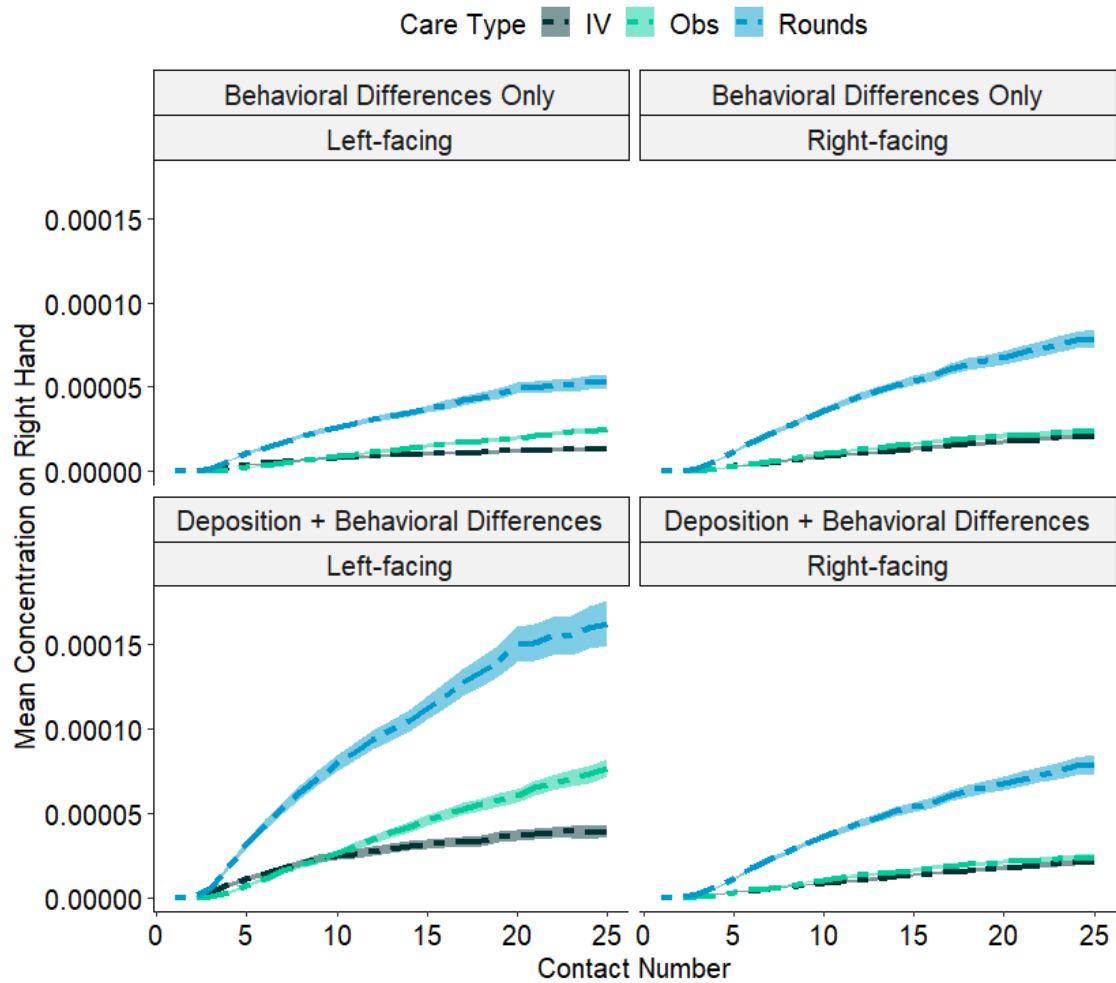
\*Please address correspondence to Amanda M. Wilson, [am.wilson@utah.edu](mailto:am.wilson@utah.edu)

933 Iteration Evaluation  
934  
935

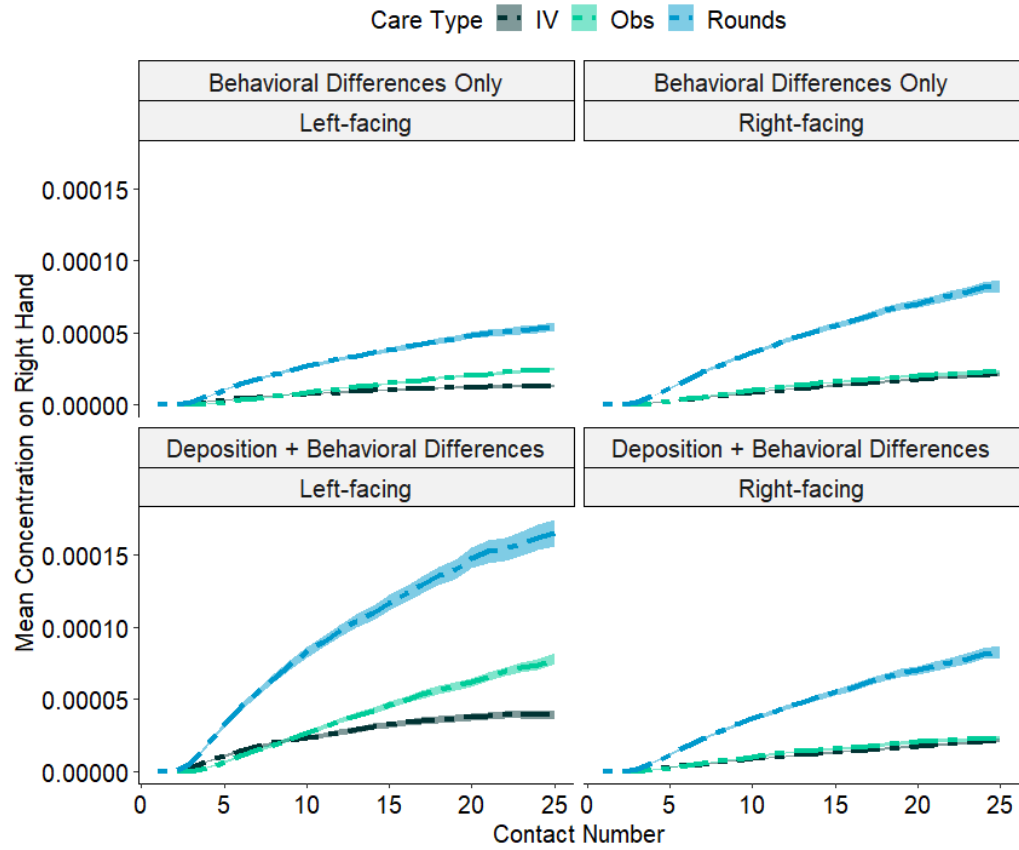


936  
937 **Figure S1.** Mean  $\pm$  SD concentration on the right hand over the number of contacts with  
938 1,000 iterations per care type and room type combination  
939

940  
941  
942  
943



944  
 945 **Figure S2.** Mean  $\pm$  SD concentration on the right hand over the number of contacts with  
 946 5,000 iterations per care type and room type combination  
 947  
 948



949  
 950  
 951  
 952  
 953

**Figure S3.** Mean  $\pm$  SD concentration on the right hand over the number of contacts with 10,000 iterations per care type and room type combination



954 *Surface Area of Surfaces*

955

956 **Table S1.** Surface area (m<sup>2</sup>) for surfaces or velocity inlet/pressure outlets

<b>Object</b>	<b>Surface Area (m<sup>2</sup>)</b>
Chair	0.24
Side table	0.25
Desk	1.5
Floor	9.5
Door	1.9
Patient	0.44
Bed	0.50
Large Window	0.18
Small Windows	0.08

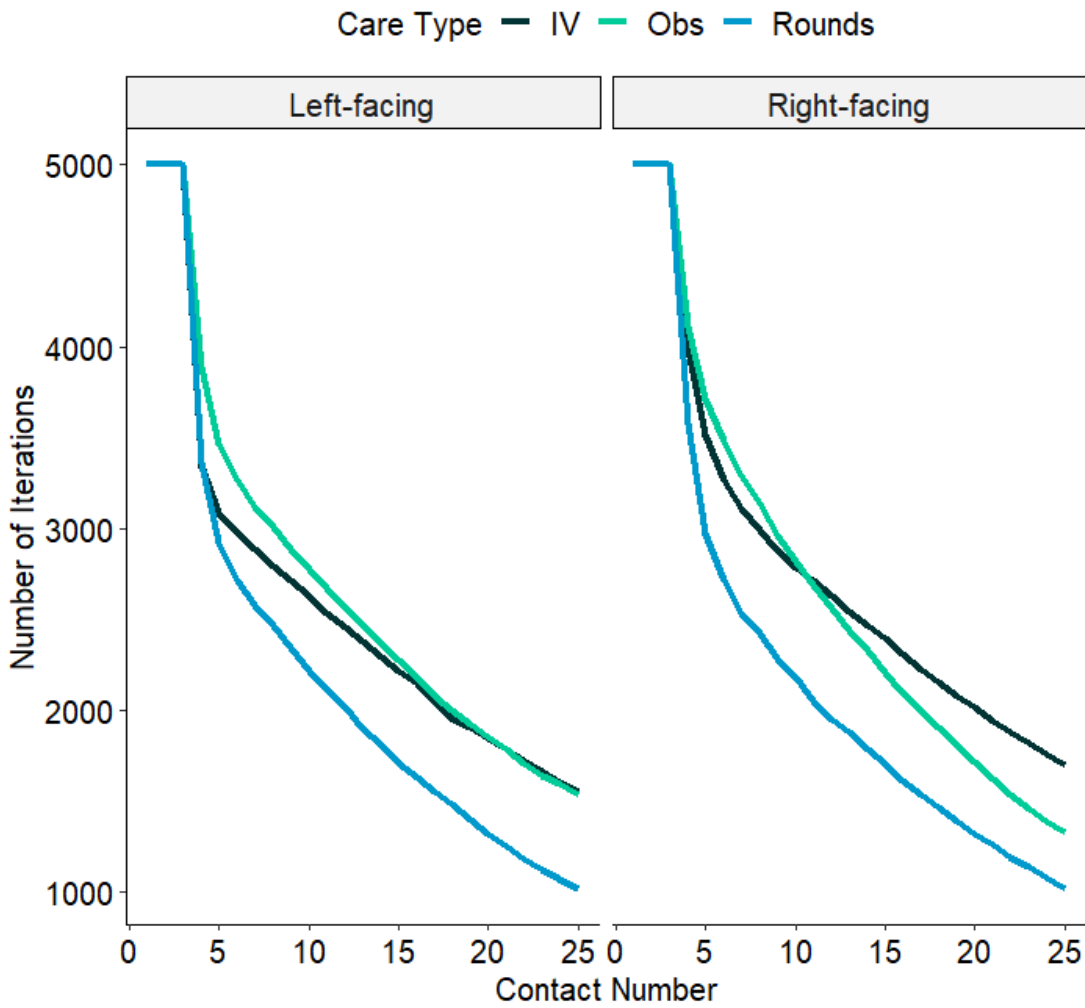
957

958

959

960

961



963  
964 **Figure S4.** Number of iterations to inform mean concentration on hands per contact  
965 number\*

966  
967 \*There is variability in length of simulations and number of contacts based on how  
968 quickly a transition to the “out” (exit from patient room) state occurs

969  
970

971 *Exposure Model Sensitivity Analysis*

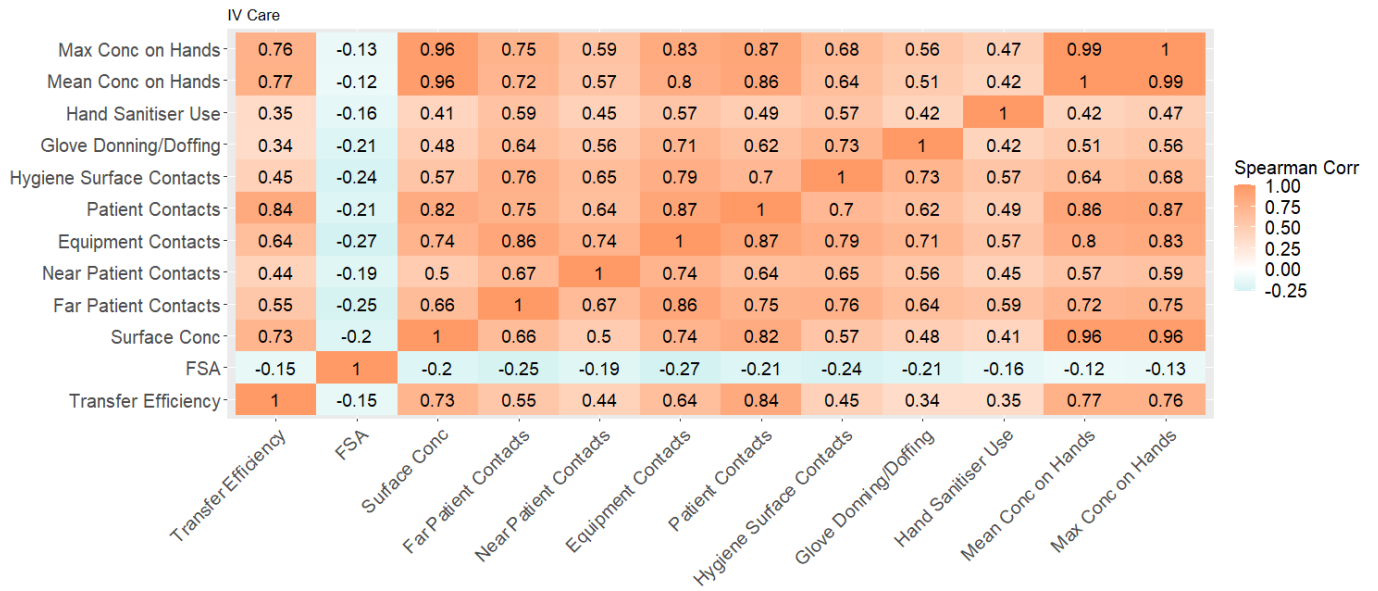
972

973 Figures S5-S22 reflect results from simulations for both deposition + behavior change  
 974 and behavior change only model scenarios.

975

976

977

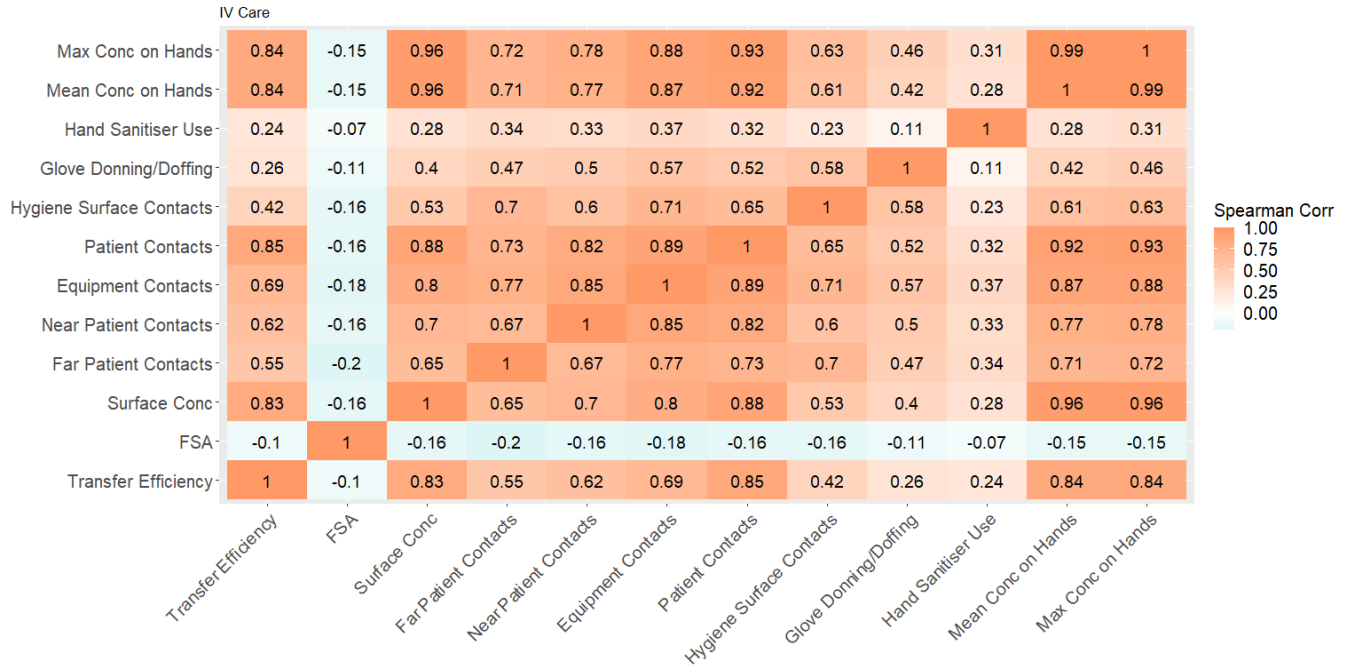


978

979 **Figure S5.** Spearman correlation coefficients for IV-care, left-facing

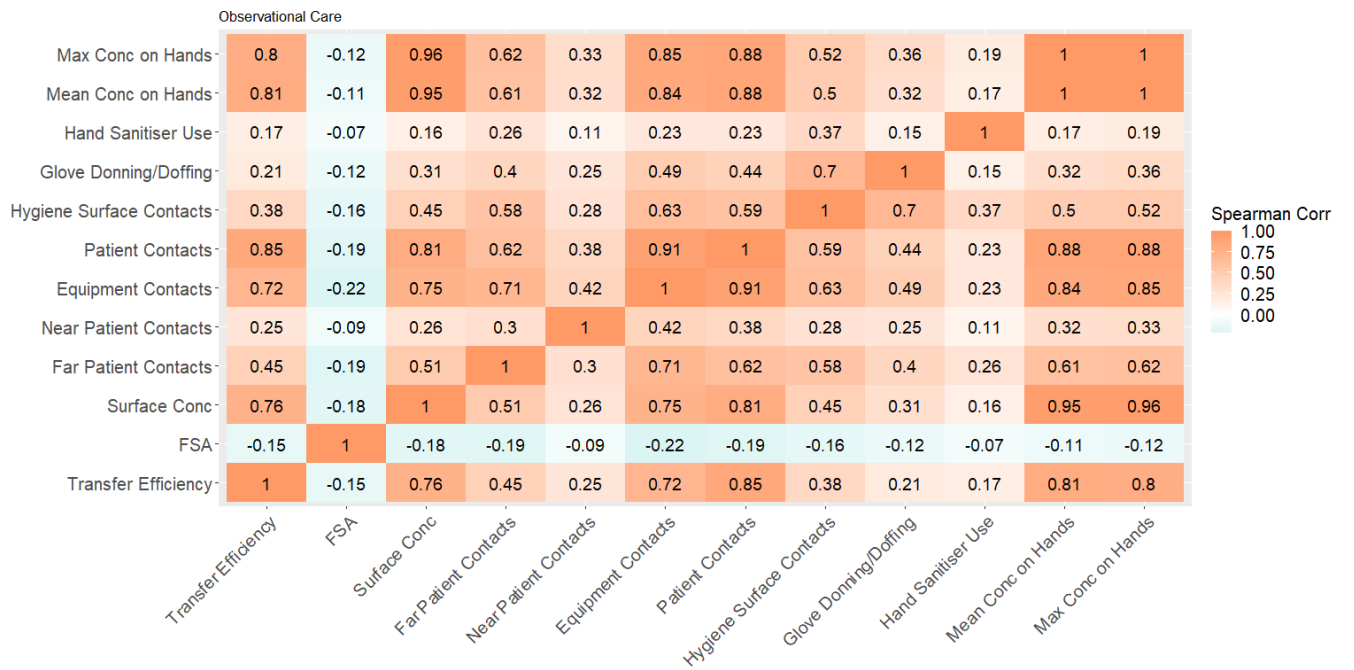
980

981



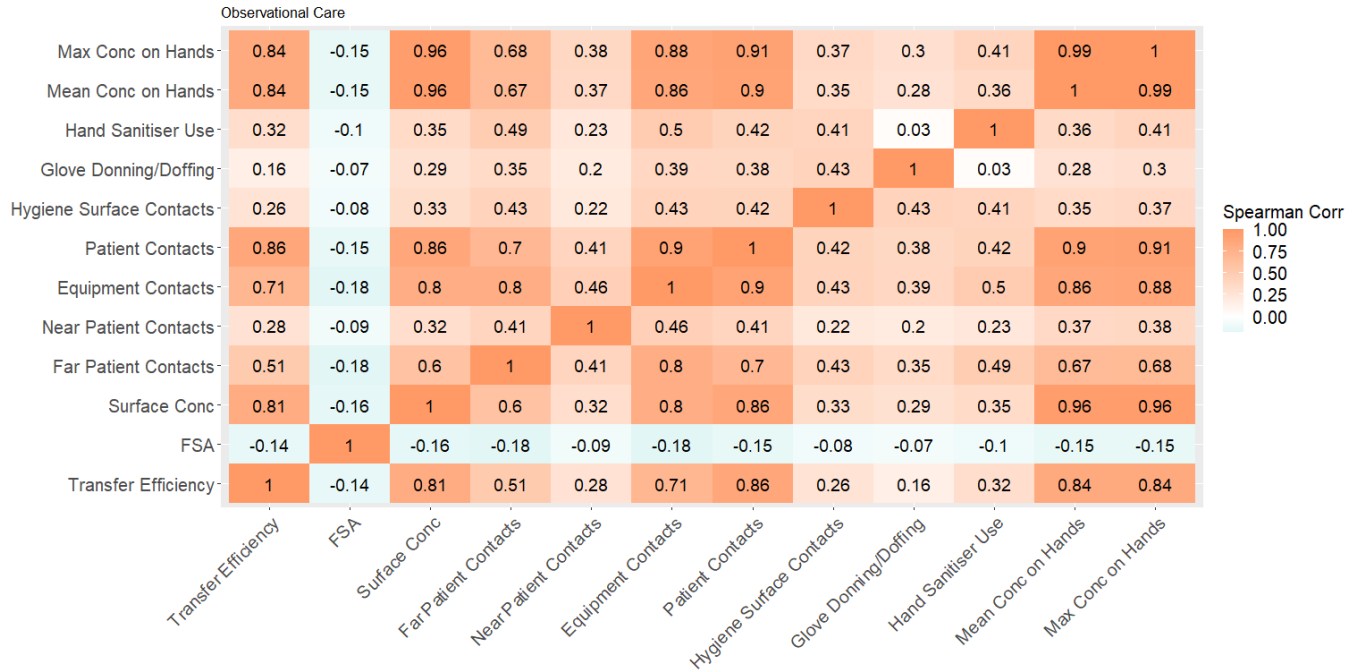
982  
 983 **Figure S6.** Spearman correlation coefficients for IV-care, right-facing

984  
 985



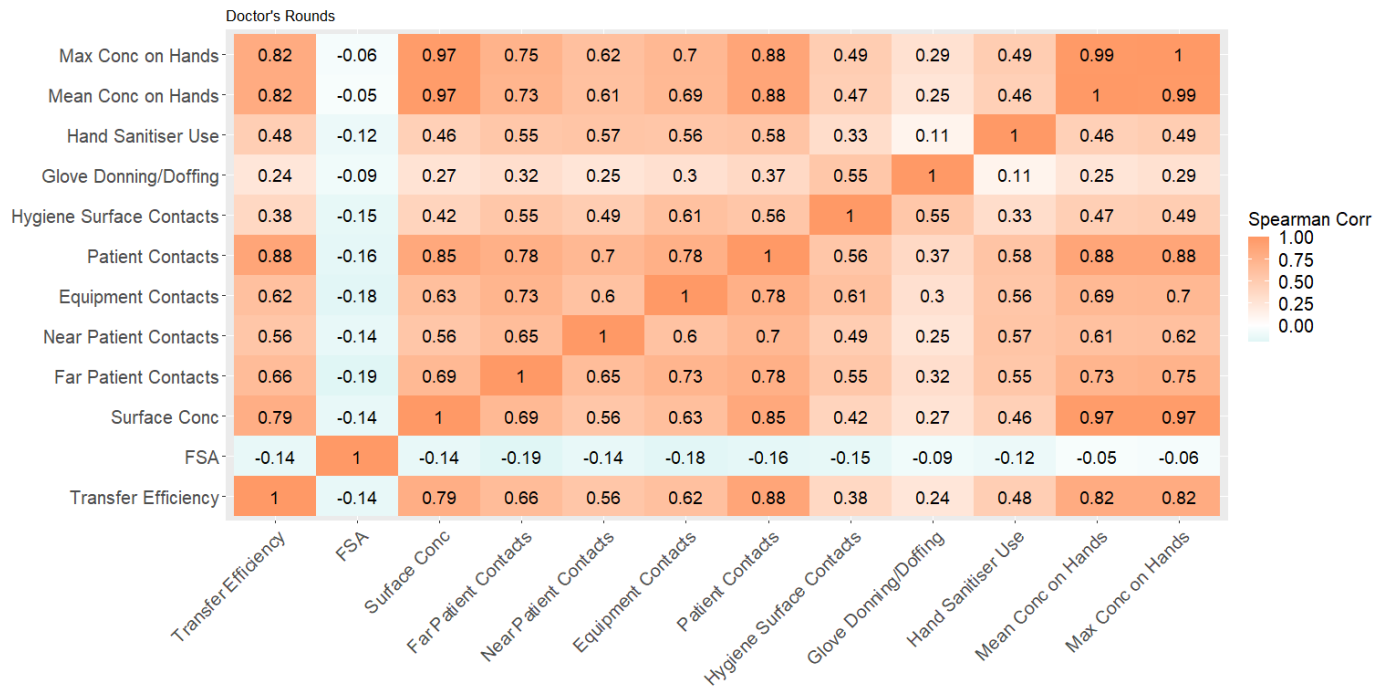
986  
 987 **Figure S7.** Spearman correlation coefficients for observational care, left-facing

988  
 989



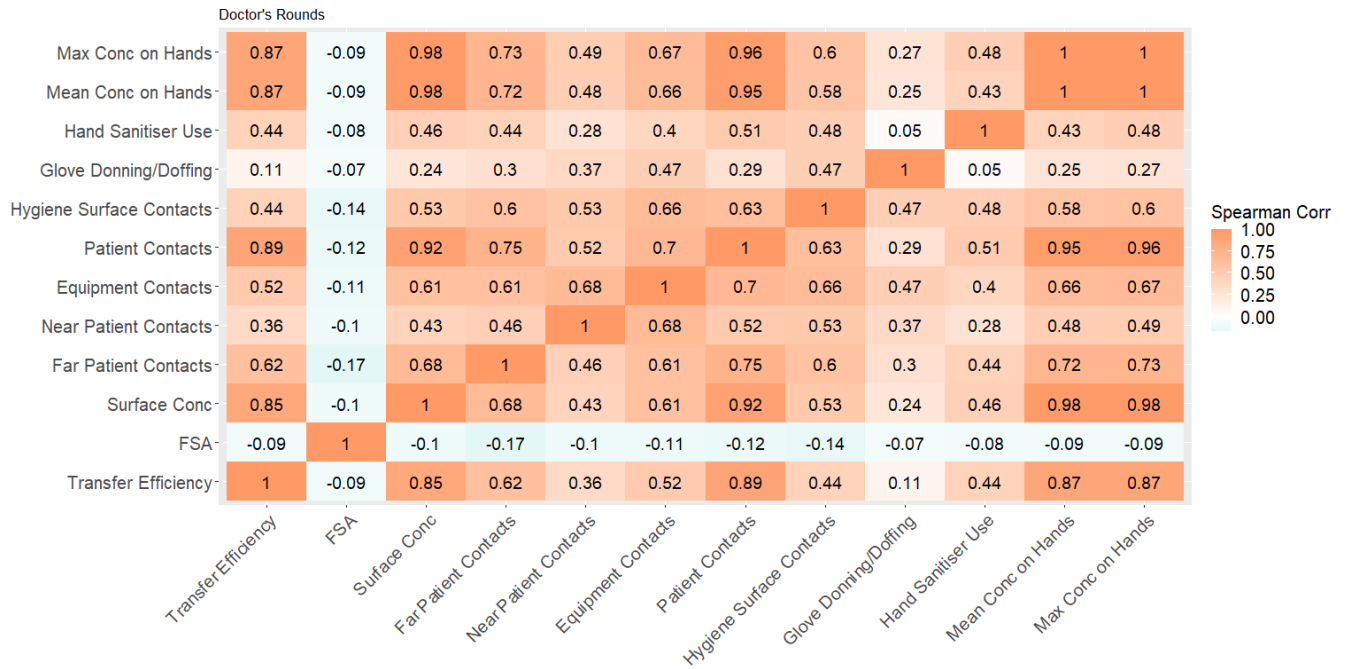
990 **Figure S8.** Spearman correlation coefficients for observational care, right-facing

991  
992  
993  
994



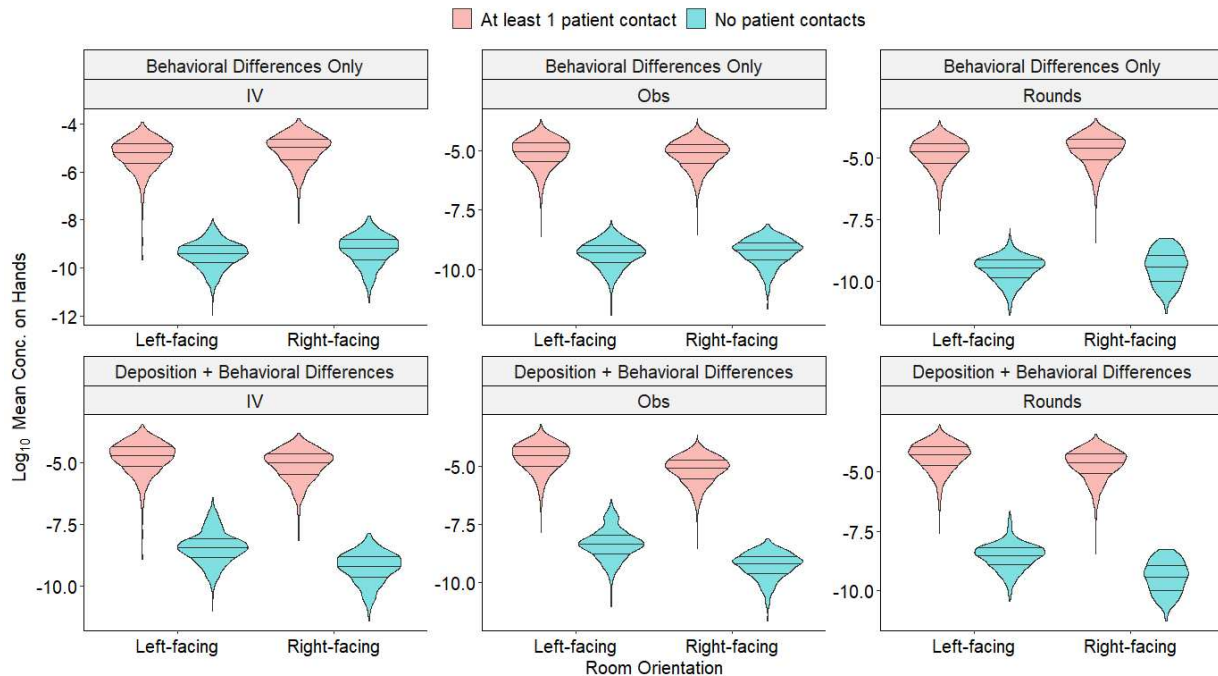
995 **Figure S9.** Spearman correlation coefficients for doctors' rounds, left-facing

996  
997



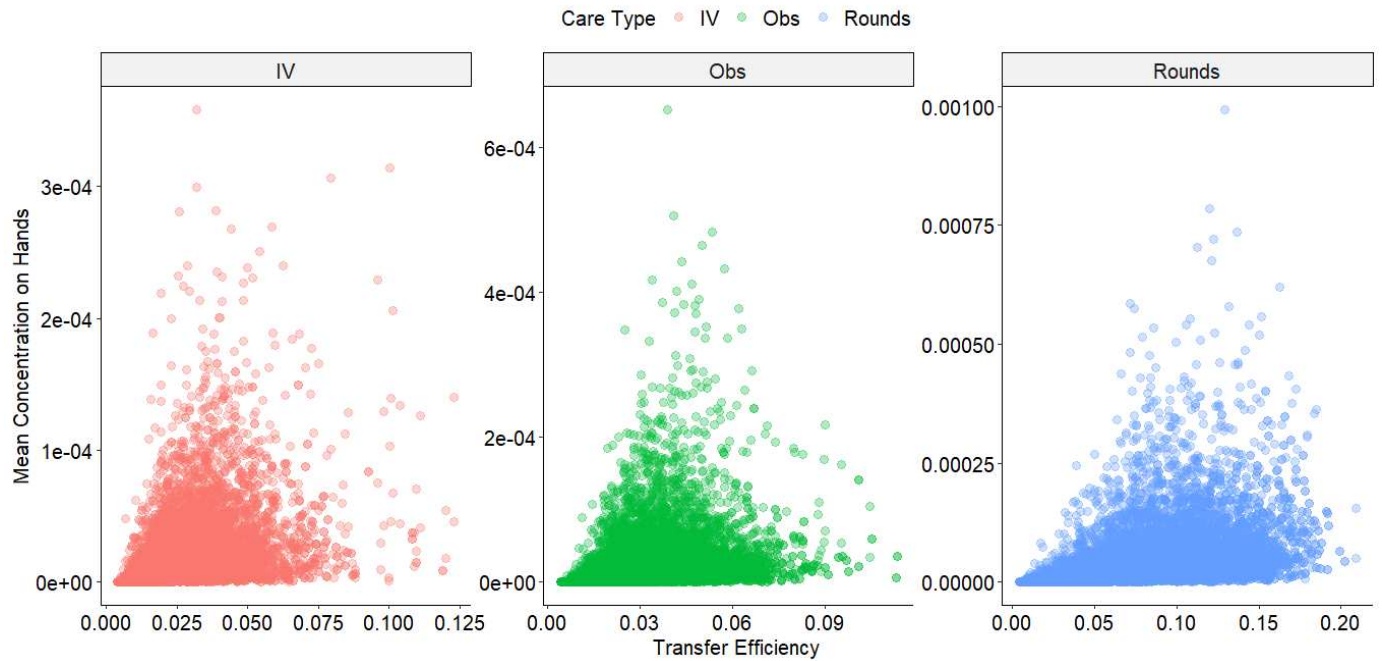
998  
 999  
 1000  
 1001  
 1002

**Figure S10.** Spearman correlation coefficients for doctors' rounds, right-facing



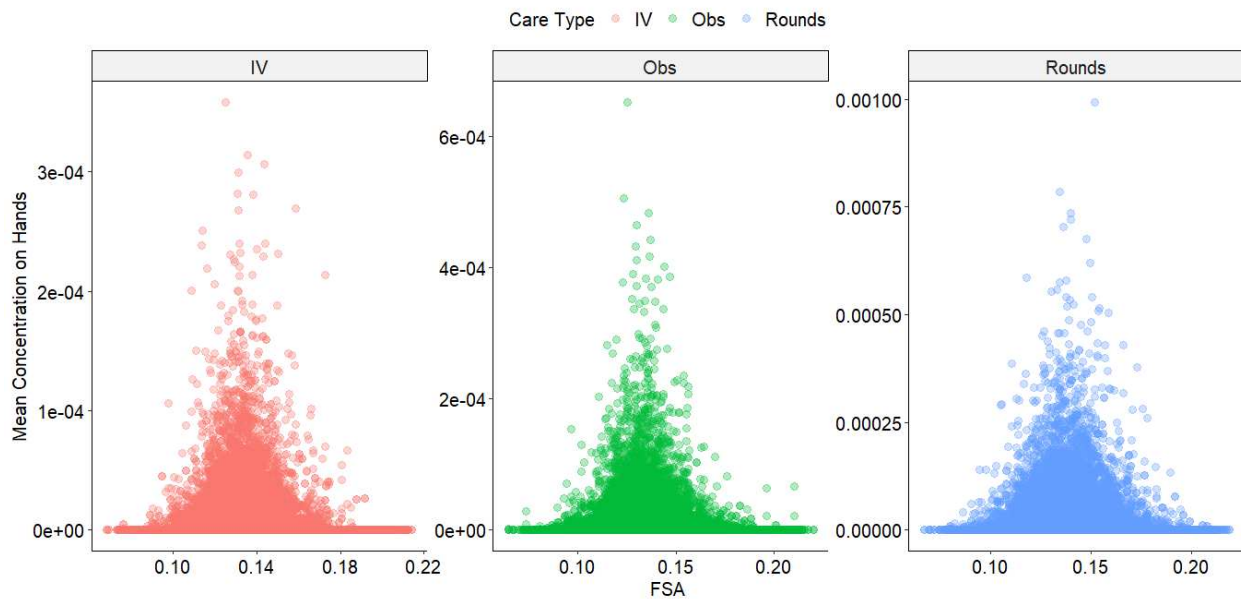
1003  
 1004  
 1005  
 1006

**Figure S11.** Distributions of Log<sub>10</sub> Mean Concentrations on Hands for All Simulations Scatter Plots



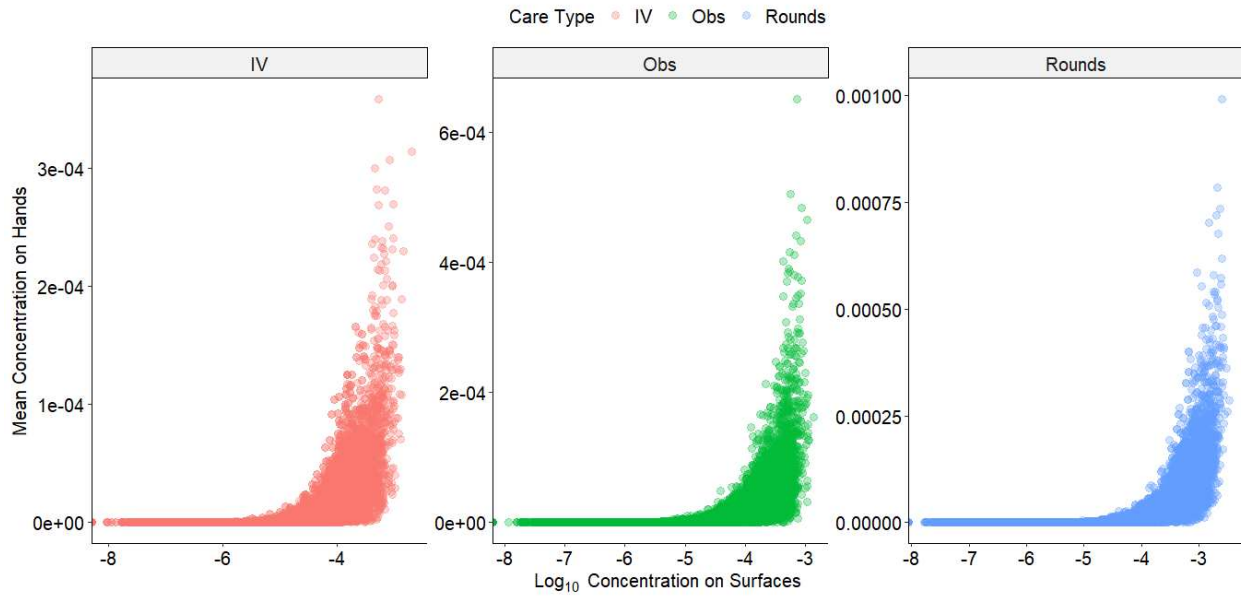
1007  
1008  
1009  
1010  
1011  
1012

**Figure S12.** Scatter plots of mean concentration on hands vs. transfer efficiency



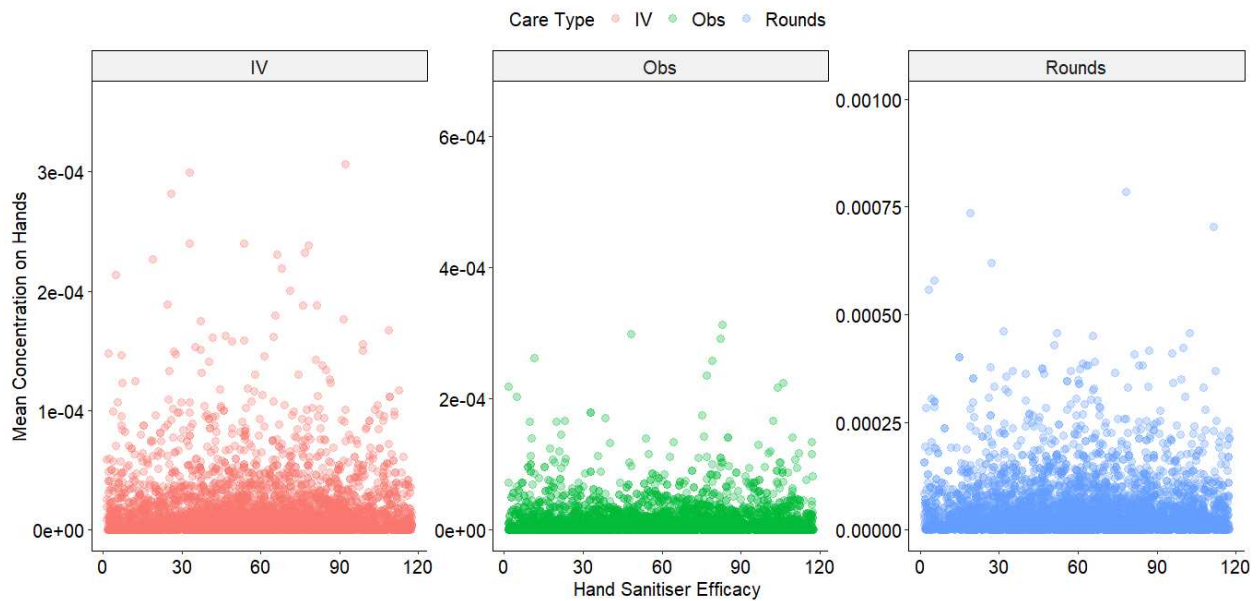
1013  
1014  
1015  
1016  
1017

**Figure S13.** Scatter plots of mean concentration on hands vs. fractional hand surface area



1018  
 1019  
 1020  
 1021  
 1022  
 1023  
 1024  
 1025

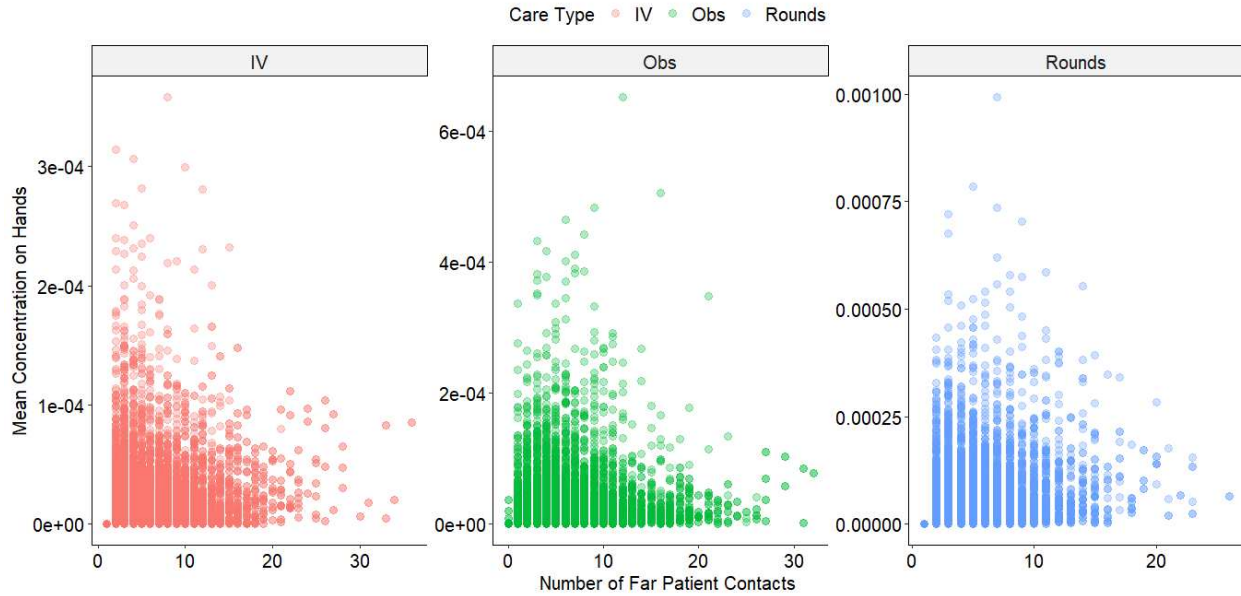
**Figure S14.** Scatter plots of mean concentration on hands vs. log<sub>10</sub> concentration on surfaces



1026  
 1027  
 1028  
 1029

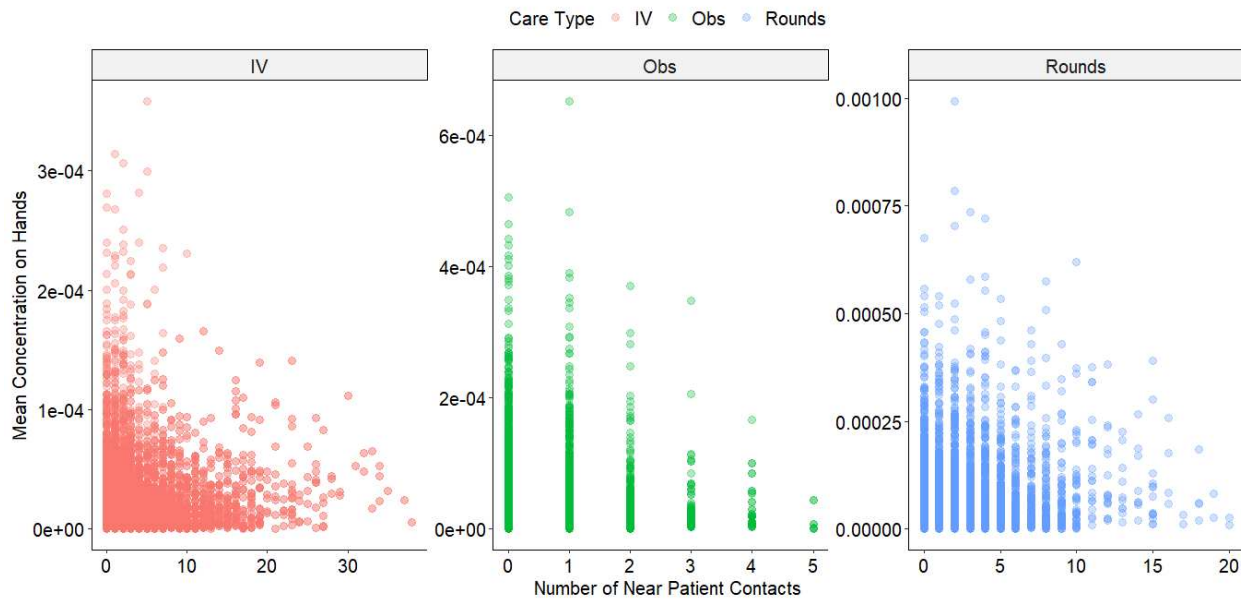
**Figure S15.** Scatter plots of mean concentration on hands vs. hand sanitizer efficacy





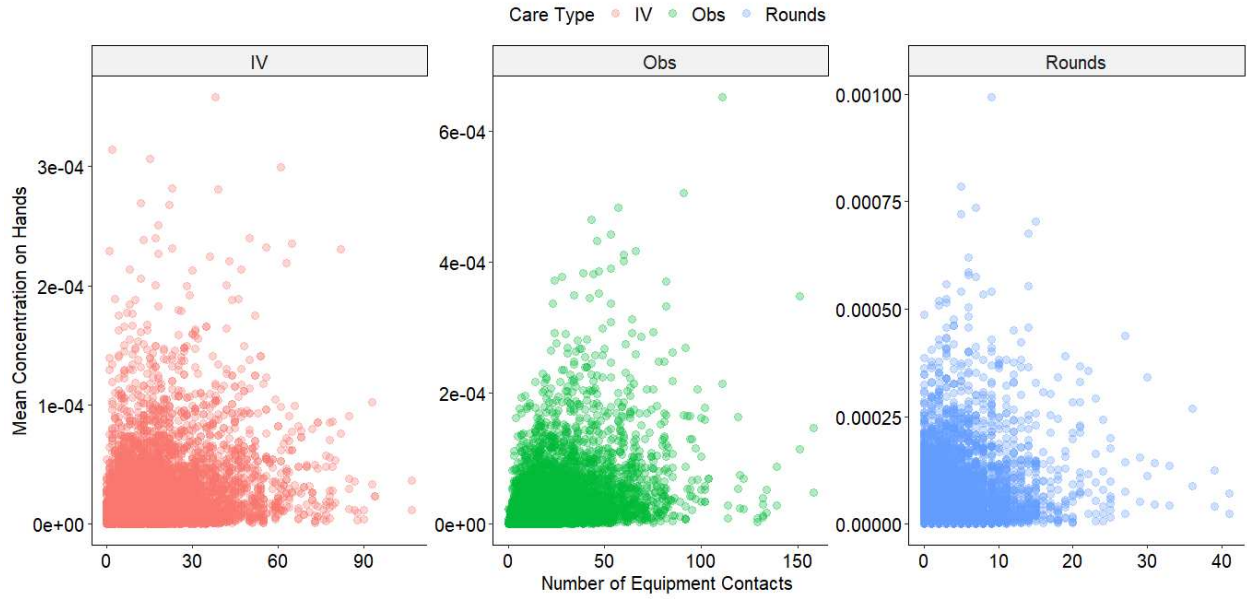
1030  
1031  
1032  
1033  
1034  
1035  
1036

**Figure S16.** Scatter plots of mean concentration on hands vs. number of far patient surface contacts



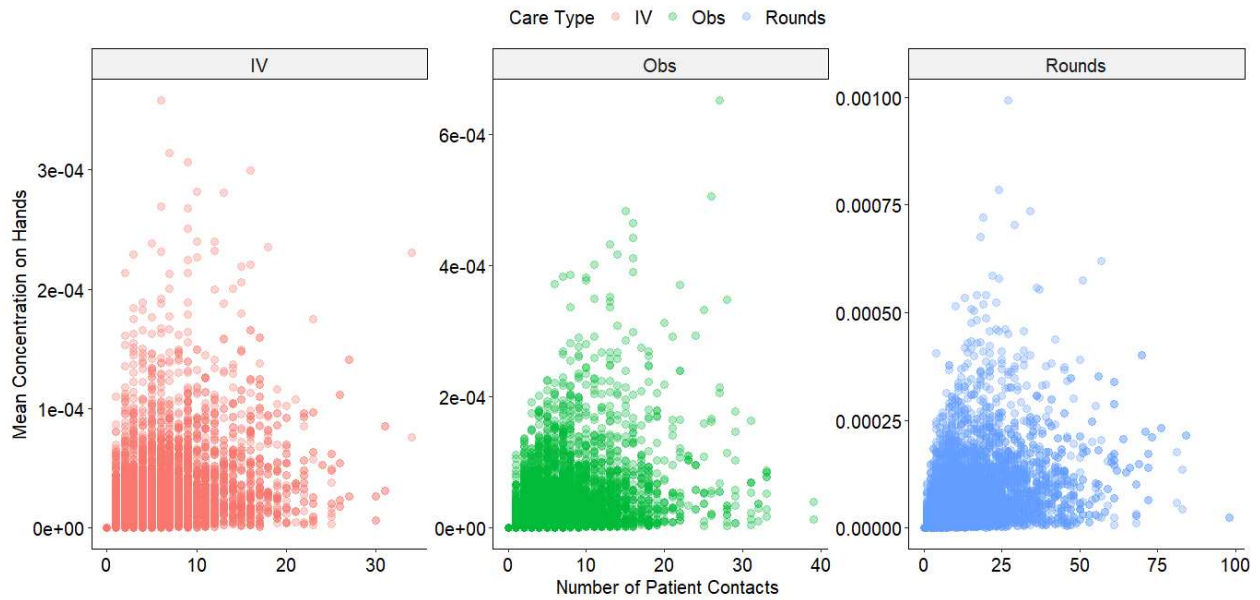
1037  
1038  
1039  
1040  
1041  
1042

**Figure S17.** Scatter plots of mean concentration on hands vs. number of near patient surface contacts



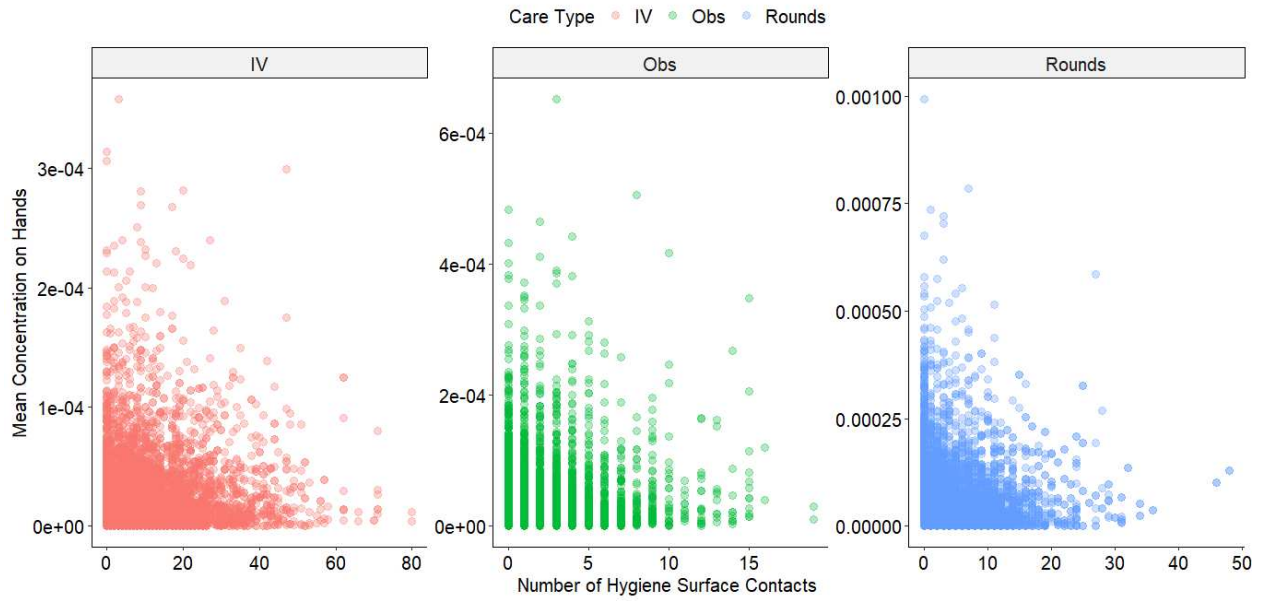
1043  
1044  
1045  
1046  
1047  
1048

**Figure S18.** Scatter plots of mean concentration on hands vs. number of equipment contacts



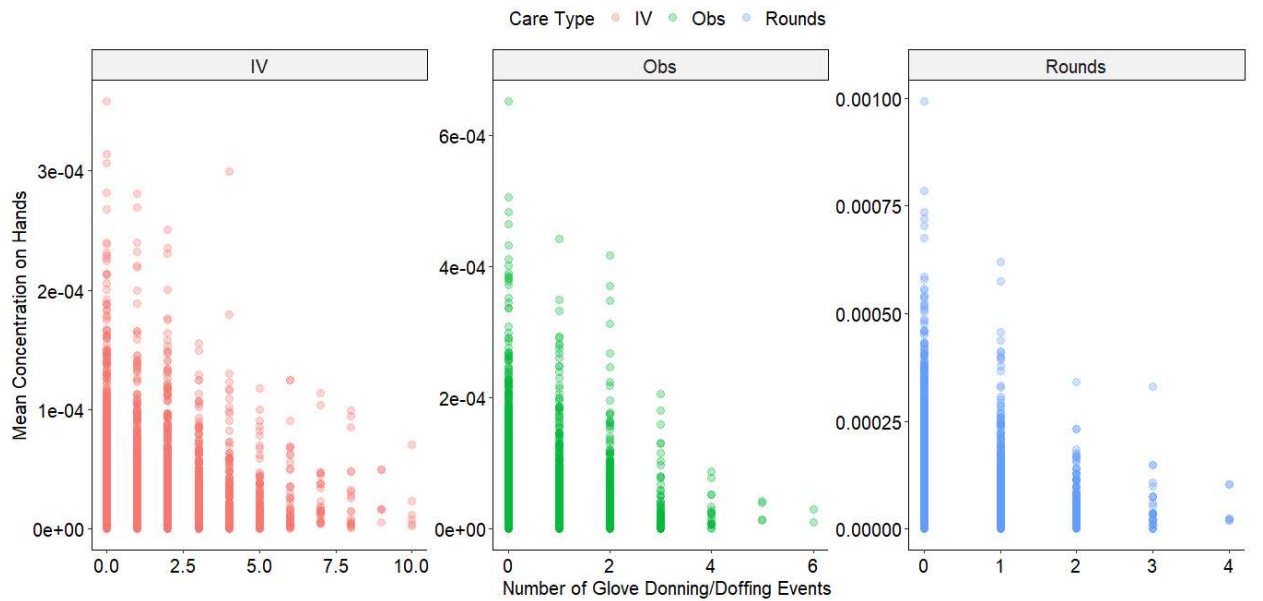
1049  
1050  
1051  
1052  
1053

**Figure S19.** Scatter plots of mean concentration on hands vs. number of patient contacts



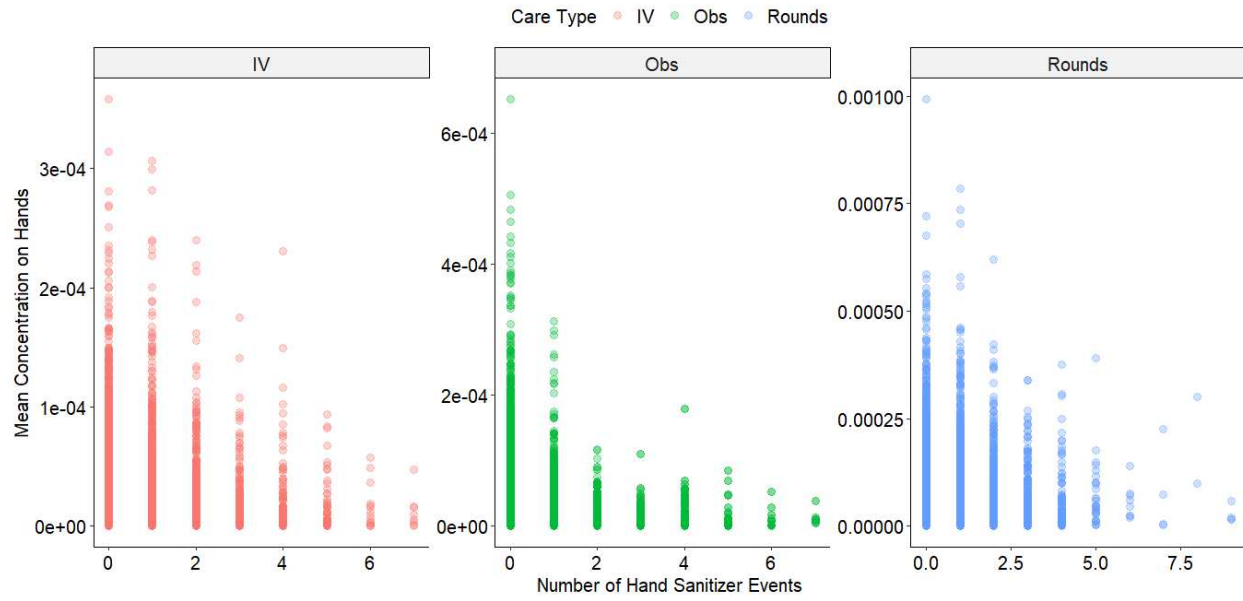
1054  
1055  
1056  
1057  
1058  
1059  
1060

**Figure S20.** Scatter plots of mean concentration on hands vs. number of hygiene surface contacts



1061  
1062  
1063  
1064  
1065

**Figure S21.** Scatter plots of mean concentration on hands vs. number of glove donning/doffing events

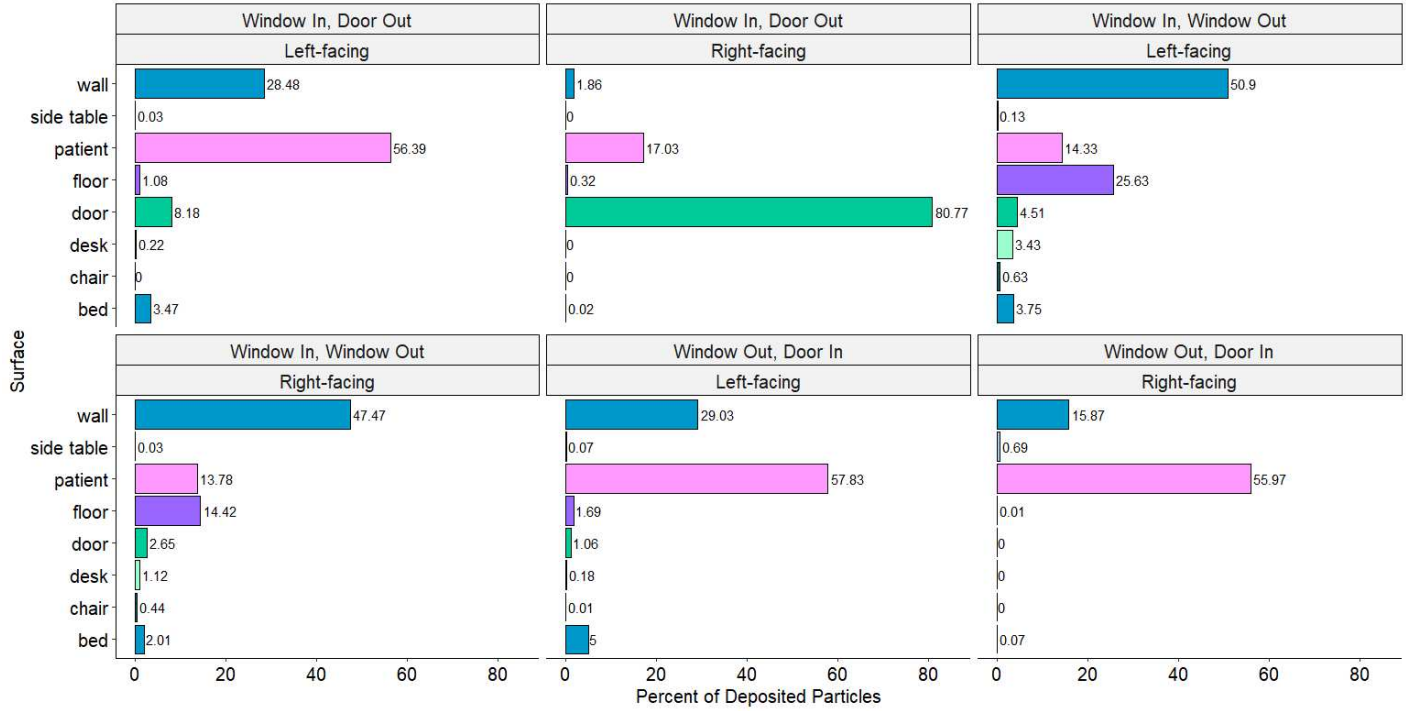


1066  
 1067  
 1068  
 1069  
 1070

**Figure S22.** Scatter plots of mean concentration on hands vs. number of hand sanitizer events

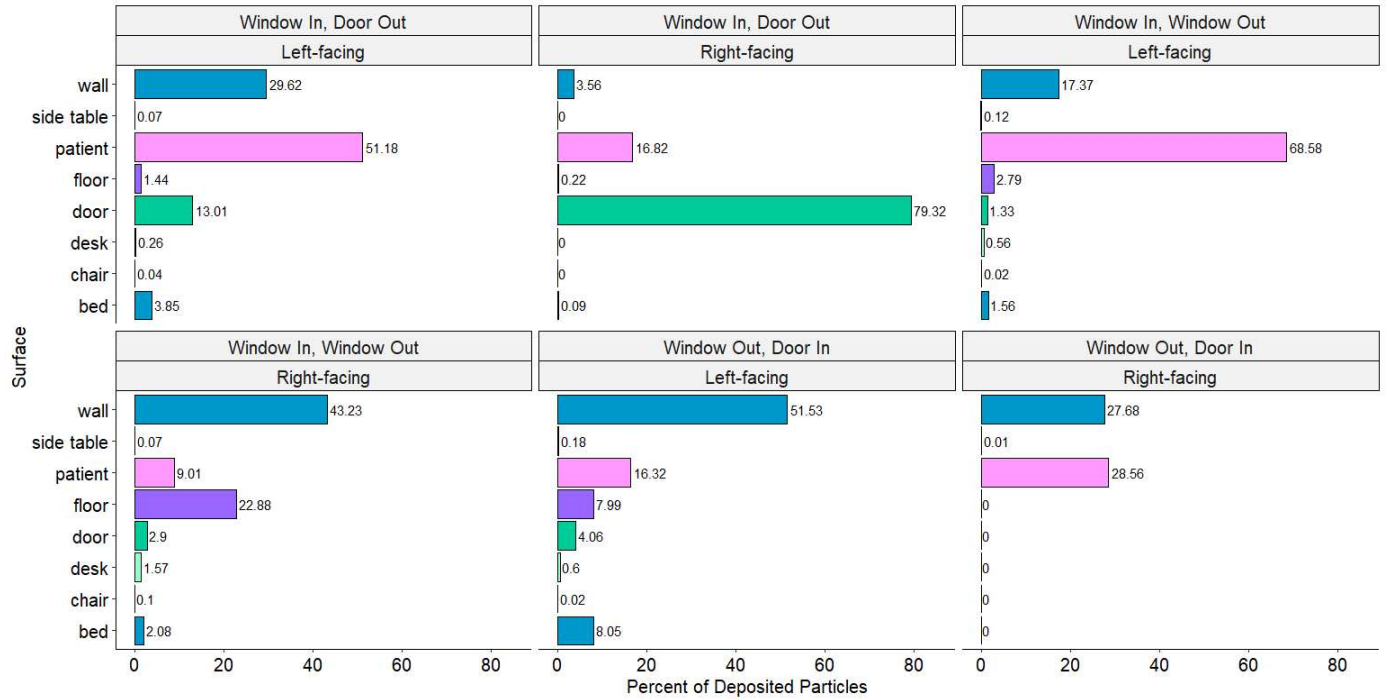
1071 *Particle Deposition Sensitivity Analysis*

1072 In some cases, proportions will not sum to 1 due to some particles exiting out of the  
 1073 windows when windows acted as pressure outlets and due to loss of particles during the  
 1074 CFD simulation.  
 1075



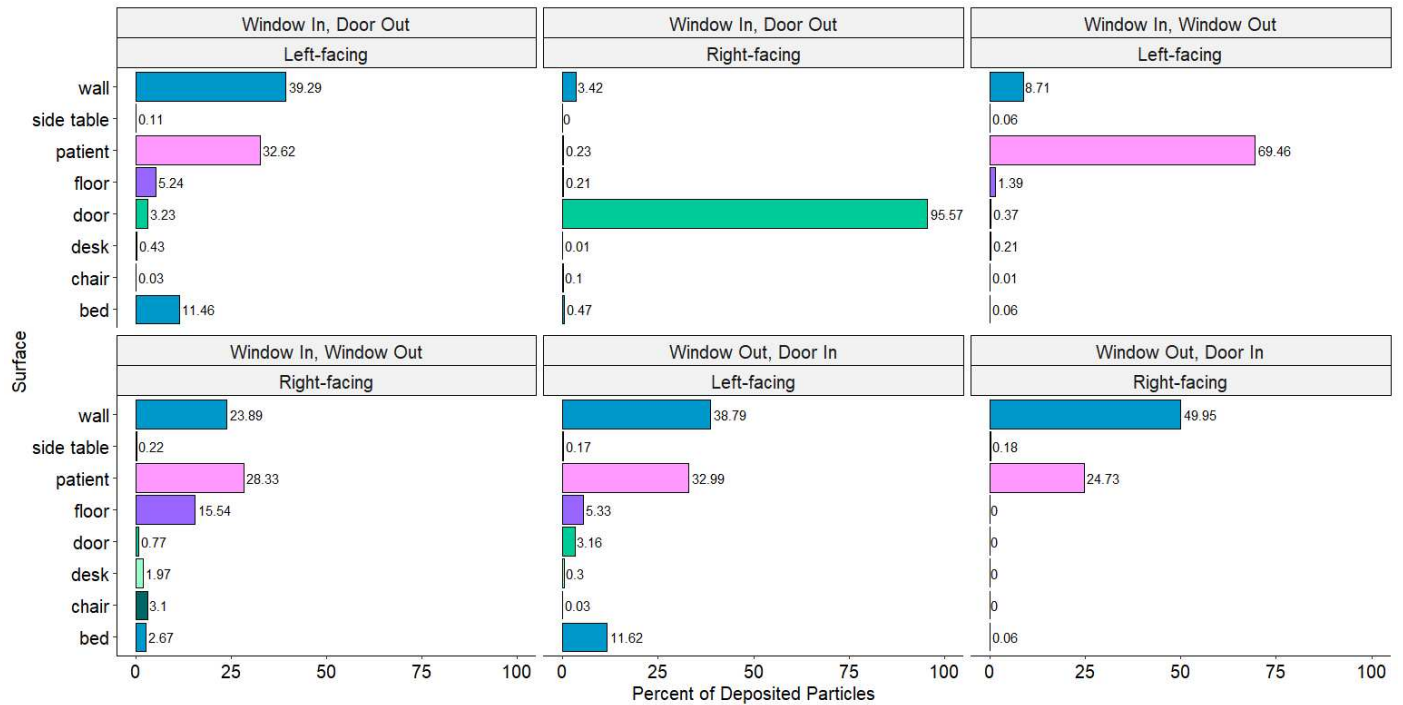
1076  
 1077 **Figure S23.** Particle deposition patterns for 10 ACH conditions  
 1078

1079  
 1080



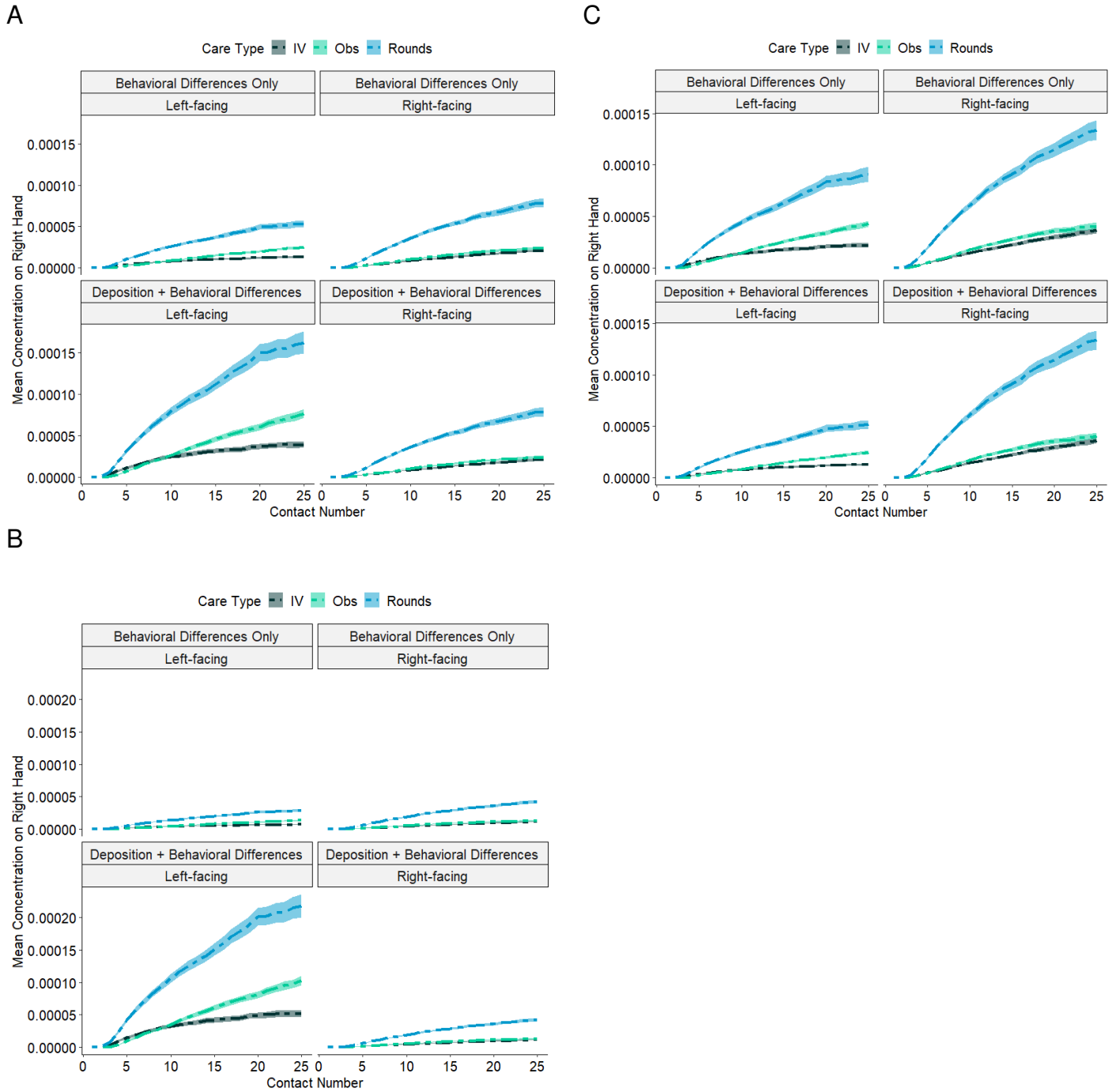
1081  
1082 **Figure S24.** Particle deposition patterns for 6 ACH conditions

1083  
1084



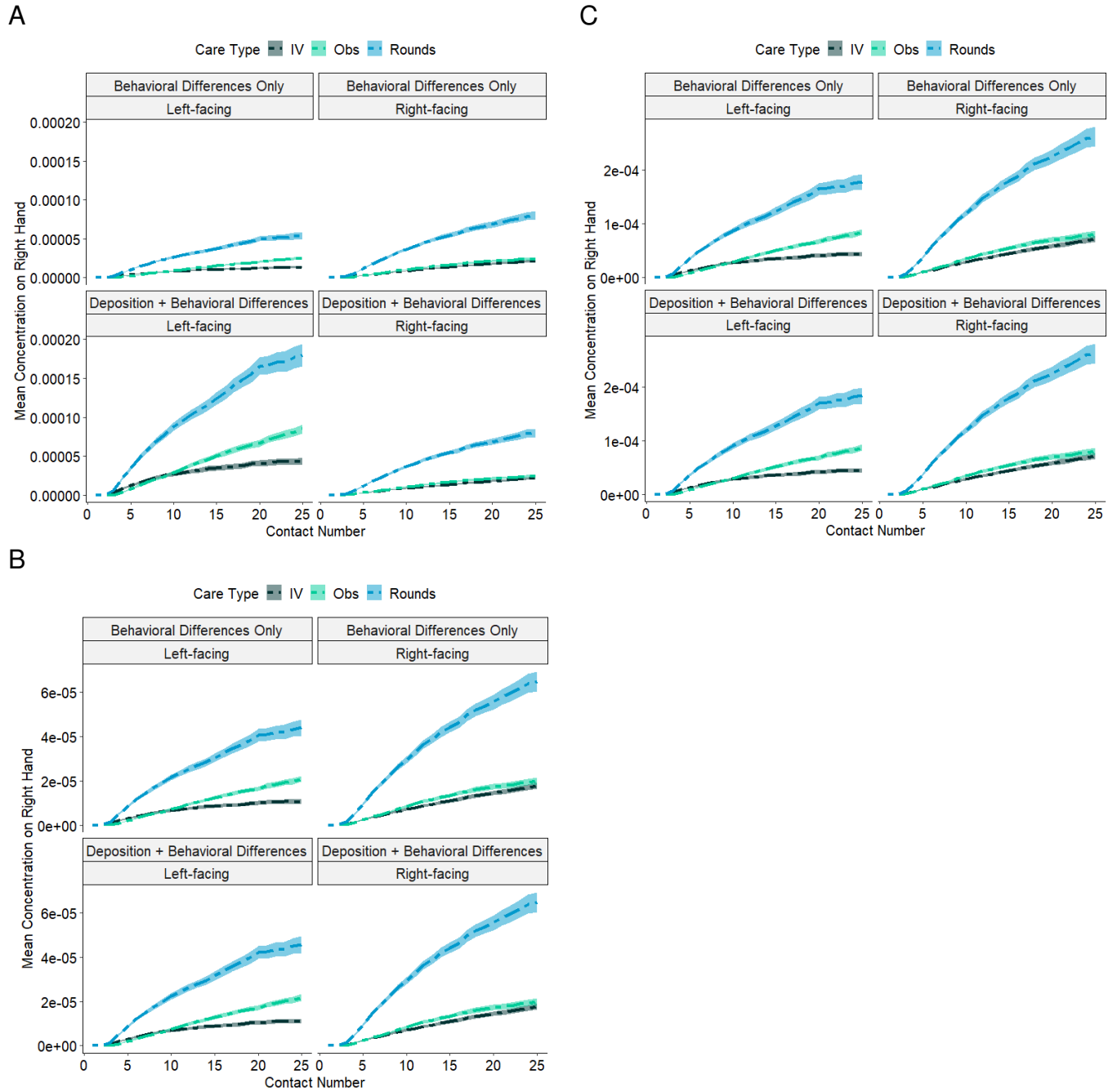
1085  
1086 **Figure S25.** Particle deposition patterns for 2.5 ACH

1087  
1088  
1089



1091  
 1092  
 1093  
 1094  
 1095  
 1096  
 1097

**Figure S26.** Mean  $\pm$  SD concentration on the right hand over the number of contacts with 5,000 iterations per care type and room type combination for **6 ACH**, A.) Window In, Door Out, B.) Window In, Window Out, C.) Window Out, Door In

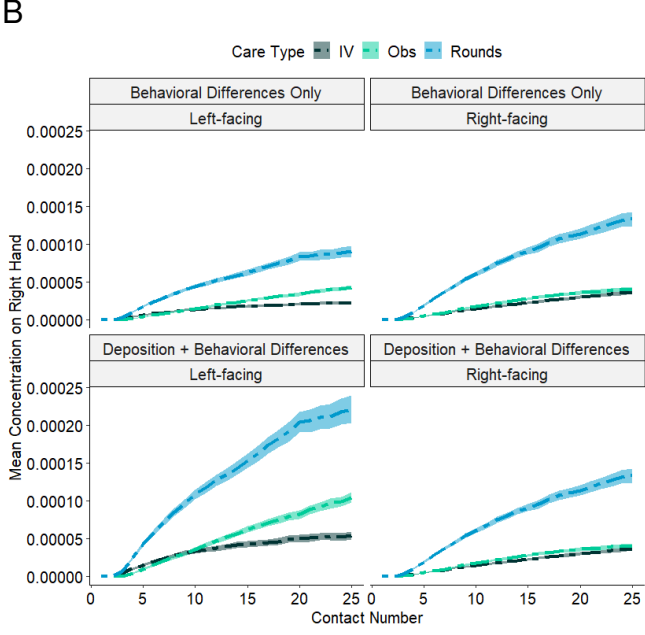
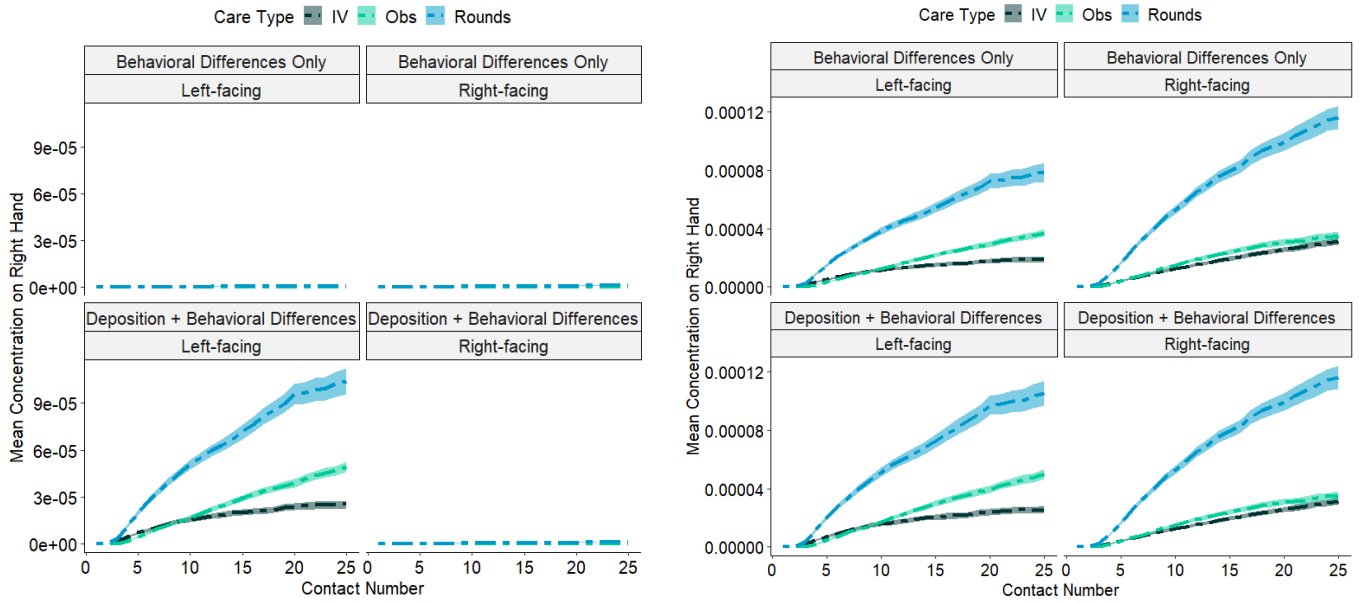


1098  
 1099  
 1100  
 1101  
 1102  
 1103  
 1104

**Figure S27.** Mean  $\pm$  SD concentration on the right hand over the number of contacts with 5,000 iterations per care type and room type combination for **10 ACH** A.) Window In, Door Out, B.) Window In, Window Out Scenario, C.) Window Out, Door In

A C





1105  
 1106  
 1107  
 1108  
 1109  
 1110

**Figure S28.** Mean  $\pm$  SD concentration on the right hand over the number of contacts with 5,000 iterations per care type and room type combination for **2.5 ACH** A.) Window In, Door Out, B.) Window In, Window Out Scenario, C.) Window Out, Door In